Published in final edited form as:
J Immunol. 2014 November 1; 193(9): 4368–4380. doi:10.4049/jimmunol.1400876.

Opposing Effects of CTLA4 Insufficiency on Regulatory versus Conventional T Cells in Autoimmunity Converge on Effector Memory in Target Tissue

Priyadharshini Devarajan[1], **Jason Miska**[1,#], **Jen Bon Lui**[1], **Dominika Swieboda**[1], and **Zhibin Chen**[1,2]

[1]Department of Microbiology & Immunology, University of Miami Miller School of Medicine, Miami, FL

[2]Diabetes Research Institute, University of Miami Miller School of Medicine, Miami, FL

Abstract

Quantitative variations in CTLA4 expression, due to genetic polymorphisms, are associated with various human autoimmune conditions, including type 1 diabetes (T1D). Extensive studies have demonstrated that CTLA4 is not only essential for the suppressive role of regulatory T (T_{reg}) cells, but also required for intrinsic control of conventional T (T_{conv}) cells. We report that a modest insufficiency of CTLA4 in mice, which mimics the effect of some human *CTLA4* genetic polymorphisms, accompanied by a T1D-permissive *MHC* locus, was sufficient to induce juvenile-onset diabetes on an otherwise T1D-resistant genetic background. Reduction in CTLA4 levels had an unanticipated effect in promoting T_{reg} cell function both *in vivo* and *in vitro*. It led to an increase in T_{reg} memory in both lymphoid and nonlymphoid target tissue. Conversely, modulating CTLA4 by either RNAi or antibody blockade promoted effector memory (T_{EM}) formation in the T_{conv} compartment. The $CD4^+$ T_{EM} cells, including those within target tissue, produced IL17 or IFNγ. Blocking IL7 signaling reduced the Th17 autoimmune compartment, but did not suppress the T1D induced by CTLA4 insufficiency. Enhanced effector memory formation in both T_{conv} and T_{reg} lineages may underpin the apparently dichotomized impact of CTLA4 insufficiency on autoimmune pathogenesis. Therefore, while the presence of CTLA4 plays a critical role in controlling homeostasis of T cells, its quantitative variation may impose diverse or even opposing effects on distinct lineages of T cells, an optimal sum of which is necessary for preservation of T-cell immunity while suppressing tissue damage.

Introduction

One of the hallmarks of the adaptive immune response is its ability to generate immunological memory against foreign antigens so as to generate a stronger immune response on secondary encounter. However, when an immune response is generated against

Correspondence: Zhibin Chen, MD, PhD, Department of Microbiology and Immunology, RMSB 3035, 1600 NW 10th Ave, Miami, FL 33136, USA. Tel: 305-243-8348; Fax: 305-243-5522; zchen@med.miami.edu.
#present address: Department of Medicine, University of Chicago

Disclosures
The authors have no financial conflict of interest.

self-antigens, immunological memory is often thought to contribute to the persistence of the autoimmune response in autoimmune diseases (1). It remains unclear how the different memory T cell subsets contribute to autoimmune damage in the target tissues.

Recent studies have shown that the basic tenets of immunological memory apply to the regulatory T cell (T_{reg}) compartment as well. During acute viral infections, it has been shown that T_{reg} cells go through the classical antigen-specific expansion, contraction and memory maintenance phases (2, 3). On secondary re-challenge, these memory T_{reg} cells are able to suppress conventional T (T_{conv}) cell responses better than naïve T_{reg} cells, thus helping to prevent excess immunopathology during a recall response. In a model of skin autoimmunity, it has been shown that memory T_{reg} cells in the tissue confer superior protection against autoimmune attack (4). Thus, T_{reg} memory in the tissue is emerging as one of the main players in regulation of autoimmune responses where persistent self-antigen expression helps in its maintenance (5).

A complex interplay of genetic factors often influences the onset of autoimmune diseases. In humans, one of the most important genetic contributors to type 1 diabetes (T1D) identified so far has been the HLA haplotype of the individual (6). Most often this genetic risk conferred by the HLA haplotype is influenced by non-HLA genetic factors such as *CTLA4* genetic polymorphisms. CTLA4 is a negative regulator of the immune system (7). *CTLA4* gene polymorphisms have also been implicated in a number of autoimmune disorders (8). Most disease-associated Single Nucleotide Polymorphisms (SNPs) of *CTLA4* have been mapped to the non-coding regions, such as promoter and 3'UTR (Untranslated Region) polymorphisms (9–12). These do not result in an ablation of CTLA4 production but rather result in a modest reduction in levels of functional CTLA4 protein (9–12) or alter the ratios of the various CTLA4 splice variants (13).

CTLA4 is expressed as multiple splice variants (7). Studies by several groups have established the function of each splice variant in various autoimmune settings (13–17). Nevertheless, the exact impact of each *CTLA4* polymorphism on T1D remains a debate. For example, one study showed that un-stimulated CD4 T cells from 14 healthy subjects had ~2–3-fold lower levels of soluble CTLA4, an effect associated with the T1D-risk +6230G alleles (13). However, a later study with 11 non-diabetic subjects including parents of T1D children did not find the linkage of +6230G>A SNP to either soluble CTLA4 or full-length CTLA4 levels if the subjects had the same −318C SNP in the promoter region of the *CTLA4* gene, but the −318C T1D-risk allele was associated with lower levels of both full-length CTLA4 and soluble CTLA4 expression (18). The discrepancy could be due to diverse ethnicity, environmental or other factors. On the other hand, the many studies associating the *CTLA4* locus with T1D have suggested a consensus theme: there is no qualitative change of mature CTLA4 protein; instead it is the modest quantitative reduction of CTLA4 that may pose a genetic risk for T1D. However, the exact impact of such quantitative changes on immune cells during T1D development remains to be characterized, especially in a disease model that reflects the human T1D onset at a juvenile age with a natural immune cell repertoire, besides the standard NOD model that has adulthood-onset diabetes with gender bias.

To model the effect of such a modest reduction in CTLA4 expression on T1D pathogenesis, we used a CTLA4RNAi mouse model (19–21). This model enabled us to study the specific influence of a modest reduction in CTLA4 coupled to a disease-susceptible *MHC* on spontaneous development of T1D, by crossing the CTLA4RNAi transgene onto the B6.H2^{g7} background. B6.H2^{g7} mice harbor the T1D-susceptible *MHC* loci from the NOD strain but with a genetic background of wild-type C57BL6 mice (22). This new model, with diabetes penetrance at juvenile age, allowed us to examine autoimmune memory T cells in target tissue during onset of T1D at young age in the animal.

In acute infectious disease settings, the CD62L^{lo}CD44^{hi} population is presumed to represent the effector memory T cell population long after antigen clearance since effector T cells are short-lived. In autoimmune settings, the CD62L^{lo}CD44^{hi} T-cell population may also include short-lived effector T cells that participate but not necessarily perpetuate autoimmune damage. Thus in the context of self-antigen persistence in autoimmunity, it is necessary to distinguish effector memory T cells from effectors by multi-parametric phenotypic analyses and functional validation. In this study we configured multi-parametric flow cytometry to identify and characterize the effector and memory compartments of the T_{conv} and T_{reg} cell subsets in the target tissue (the pancreas) and the draining lymph nodes. We also sought to target the autoimmune memory T cell compartment in the new early-onset T1D model by blocking IL7 signaling (23, 24).

Materials and Methods

Mice

B6.NOD-(*D17Mit21-D17Mit10*)/LtJ, Foxp3^{FIR}, *Foxp3^{sf}*, BDC2.5, CTLA4RNAi knockdown transgenic and PL4 vector control transgenic mice were described previously (19–22, 25–28). CTLA4RNAi and PL4 transgenic lines, originally generated on the NOD genetic background (19), were crossed onto the C57BL/6 (B6) background (20, 21) and then crossed with a congenic line, B6.NOD-(*D17Mit21-D17Mit10*)/LtJ (the Jackson laboratory, Bar Harbor, ME) (22), to generate the CTLA4RNAi transgenic line on the B6 genetic background but carrying a diabetes-susceptible *MHC* locus, *H2^{g7}*. Of note, the CTLA4RNAi transgenic line was established with the third-generation lentiviral vector system. The transgenic integrate contains the lentiviral vector backbone with a self-inactivating LTR but not genes for viral protein products (19). The transgenic line exhibited *MHC*-dependent site-specific immune damage, without signs of type 1 interferon responses or systemic immune activation or systemic inflammation responses (19). We did not find significant differences between the PL4 lentiviral vector control transgenic mice and transgene-negative controls including potential type 1 interferon response, T-cell activation status and histopathology of major organs surveyed in the animals (19). For controls, we used age-matched PL4 transgenic mice or the transgene-negative littermates of the CTLA4RNAi transgenic mice. The former serves better if the GFP marker is needed (for imaging or flow cytometry). The latter serves better for the autoimmune disease development in CTLA4RNAi mice because it controls the environmental factors as well as the effect of microbiota which is primarily derived from birth mothers.

We should emphasize that although the B6.NOD-(*D17Mit21-D17Mit10*)/LtJ congenic line was referred to as "B6.H2^{g7}", this nomenclature is oversimplified. The B6.NOD-(*D17Mit21-D17Mit10*)/LtJ congenic line on the B6 background carries a 19 cM segment of Chromosome 17 extending from *D17Mit21* through *D17Mit10* that includes the major histocompatibility complex, *H2*, of NOD origin. However, that segment may also contain non-*MHC*-related T1D-susceptibility or -resistant loci that are difficult to define because of the strong linkage disequilibrium to the *MHC*-related genes. Of note, the CTLA4RNAi experiments with the animals on the B6.H2^{g7} genetic background used transgene-negative littermate controls only. Although it would be ideal to have the PL4 transgenic line on the B6.H2^{g7} genetic background as additional controls, we did not generate a new line of PL4/B6.H2^{g7} animals due to the costs involved. The transgene-negative littermate controls, as discussed previously, were deemed adequate since the PL4 transgenic line did not promote autoimmune damage to the pancreas in the NOD model (19), in the BDC2.5/NOD model or on the B6 genetic background (see Results below).

BDC2.5/NOD.Foxp3^{FIR} mice were generated by crossing BDC2.5/NOD with NOD.Foxp3^{FIR} mice (20, 21). The CTLA4RNAi transgenic line carries a lentiviral shRNA transgene targeting a 3'UTR region shared by all spice variants of CTLA4. It reduced CTLA4 expression 2–3 fold in both the T_{reg} and T_{conv} compartments (19). IL17A knockout B6.IL17^{-} mice (29) (the Jackson laboratory) were crossed with CTLA4RNAi/B6 mice to generate CTLA4RNAi/B6.IL17^{-} mice. The studies were approved by the Institutional Animal Care and Use Committee at the University of Miami. All animals were maintained in a specific-pathogen-free barrier facility.

Diabetes monitoring and insulitis scoring

Monitoring of diabetes incidence by urine and blood glucose measurement and assessment of immune damage in the pancreatic islet by histopathology examination were conducted according to standard procedures (21, 28).

Liver histology scoring

Inflammatory infiltration was scored based on the extent of infiltration around blood vessels (including the central vein, portal vein and the hepatic artery) and sinusoids. Each blood vessel/sinusoid was scored for inflammatory infiltration around it and the total score was averaged to assign a score to the liver (0, no lymphocytic infiltration; 2, light infiltration; 4, medium infiltration; 6, heavy infiltration).

Isolation of cells from the pancreas

Mouse pancreata were cut into small pieces (<2mm) and incubated in RPMI media containing 55% fetal bovine serum in a petri dish at 37°C with 5% CO_2 for 3–4hrs, immediately after dissection from the mouse. The mouse was either perfused with PBS or the pancreatic tissue was blotted and washed with PBS, to remove lymphocytes from the blood circulation. After 3–4hrs, the pancreas debris was removed, and the cells in the media were collected from the petri dish, filtered with a 70um cell strainer, and analyzed.

Flow cytometry

Single cell suspensions of spleens and lymph nodes were prepared for staining. The cells were then blocked using anti-CD16/32 (2.4G2) and normal mouse serum (Jackson ImmunoResearch, West Grove, PA). The cells were then stained for surface markers with antibody conjugates. The following fluorescently labeled antibody conjugates were used: CD4- PECy7, CD8-Brilliant Violet 605, CD44-Brilliant Violet 785, CD127-Biotin (BioLegend, San Diego, CA); CD8-APCeFluor780, CD3-AlexaFluor700, CD44-eFluor450, CD62L-APC, CD62L-APCeFluor780, CD69-PE, Streptavidin PerCp-eFluor710, PD-1-eFluor450 (eBioscience, San Diego, CA); CD4-V500 (BD Biosciences, San Diego, CA); CD4-PE-Texas Red (Invitrogen, San Diego, CA). For intracellular Foxp3 staining, cells were fixed and permeabilized with reagents in the Foxp3 staining kit (eBioscience) and then stained intracellularly with Foxp3-eFluor450 (eBioscience). Cells were then analyzed using a LSRII flow cytometer with FACSDiva software (BD Biosciences).

For intracellular cytokine staining, single cell suspensions of cells were prepared in cRPMI. 4 million cells/ml were re-suspended in stimulation media (cRPMI+ 40nM PDBu + 2uM ionomycin) and incubated at 37°C for 6 hours. Brefeldin A (eBioscience) was added 30–60 minutes after beginning of incubation. The cells were then collected and stained for surface markers. The cells were then fixed with 2% PFA for 30minutes. This was followed by permeabilization using the Perm/Wash buffer (BD Biosciences). For intracellular cytokine staining the following antibodies were used: IFNγ-PECy7 (BioLegend, CA), IL17A-eFluor450, IFNγ-APC, IL17A-PECy7 (eBioscience).

A gating strategy was developed for analyses of the effector and memory subsets. T_{conv} cell compartment was first gated on $CD3^+CD8^-CD4^+Foxp3^-$ (for $CD4^+$ T cells) or $CD3^+CD8^+CD4^-$ (for $CD8^+$ T cells), and then analyzed for central memory T cells (**T_{CM}**) ($CD44^{hi}CD62L^{hi}$), effector memory T cells (**T_{EM}**) ($CD44^{hi}CD62L^{lo}CD127^+CD69^-$), and effector T cells (**T_{EFF}**) ($CD44^{hi}CD62L^{lo}CD127^-CD69^+$). T_{reg} cell compartment was analyzed for T_{reg} effector memory cells (**$T_{reg\text{-}EM}$**) ($CD3^+CD8^-CD4^+Foxp3^+CD44^{hi}CD62L^{lo}CD127^+CD69^-$) and T_{reg} effector cells (**$T_{reg\text{-}EFF}$**) ($CD3^+CD8^-CD4^+Foxp3^+CD44^{hi}CD62L^{lo}CD127^-CD69^+$). To analyze intracellular cytokine profiles, cell populations were: first gated on $CD3^+CD8^-CD4^+$ (for $CD4^+$ T cells) or $CD3^+CD8^+CD4^-$ (for $CD8^+$ T cells) and then analyzed for T_{EM} ($CD44^{hi}CD127^+$) and T_{EFF} ($CD44^{hi}CD127^-$).

Cell sorting and adoptive transfer

For *in vivo* T_{reg} suppression experiments: donor splenocytes of PL4/B6.$Foxp3^{FIR}$ control mice or CTLA4RNAi/B6.$Foxp3^{FIR}$ were used to purify $Foxp3^{FIR+}$ T_{reg} cells using the RFP marker. Naïve T_{reg} ($CD4^+CD62L^{hi}Foxp3^{FIR+}$) cells were sorted using a FACSAria II flow cytometer (BD Biosciences, San Diego, CA). 200,000 sorted T_{reg} cells from donor mice were re-suspended in PBS and injected intraperitoneally into 2–3 day old Foxp3-deficient B6.*Foxp3*^{sf} recipients. Donor T_{reg} cells were also marked with ubiquitously expressed GFP by the lentiviral transgene. To examine *in vivo* suppression of adoptively transferred T_{reg} cells, the T_{reg}-reconstituted B6.*Foxp3*^{sf} mice were sacrificed at 2–3 weeks of age and T cell activation was analyzed by flow cytometry.

For adoptive transfer studies of T_{EM} and T_{EFF} cells of the T_{conv} compartment, donor splenocytes from BDC2.5/NOD.Foxp3^{FIR} mice were processed and stained as described above. $CD4^+$ T_{EM} or $CD4^+$ T_{EFF} cells were sorted using a FACSAria II flow cytometer (BD Biosciences). 50,000 sorted $CD4^+T_{EM}$ or $CD4^+$ T_{EFF} cells from donor mice were injected intravenously into 3–5 week old NOD.SCID recipients. These mice were then monitored for diabetes and at the end point were analyzed by flow cytometry. For lymphoreplete transfer experiments, 200,000 $CD4^+$ T_{EM} or $CD4^+$ T_{EFF} cells sorted from BDC2.5/NOD.Foxp3^{FIR} mice were injected intravenously into adult CD90.1 congenic NOD recipients. These mice were sacrificed 5–6 days after transfer and were analyzed by flow cytometry.

T_{reg} in vitro suppression assay

$CD4^+CD25^+$ Regulatory T Cell Isolation Kit (Milteyni Biotec, San Diego, CA) was used to isolate $CD4^+$ T_{reg} cells and T_{conv} cells. 100,000 T_{conv} cells were stimulated with 100,000 irradiated APCs and 0.5ug/mL purified anti-CD3 (eBioscience, San Diego, CA) for 72 hours in a 96 well round-bottom tissue culture plate. Isolated T_{reg} cells were titrated at T_{reg}:T_{conv} ratios of 1:1, 1:2, 1:4, 1:8 and 1:16. The culture was pulsed with [^{3}H] thymidine for the last 16 hours. The amounts of incorporated ^{3}H were measured by β-counter (1450 LSC and Luminescence counter, PerkinElmer, Boston, MA). Suppression was calculated as the % reduction in CPM compared to the T_{conv} proliferation on stimulation with no T_{reg} cells added.

Antibody treatment

Anti-CTLA4 (UC-10) and anti- IL7 receptor α (IL7Rα, CD127) (clone A7R34) (23) antibodies for *in vivo* blocking experiments were purified from hybridoma cell culture. BDC2.5/NOD/Foxp3^{FIR} mice were intraperitoneally administered with anti-CTLA4 (UC-10) antibody or Hamster IgG control antibody (Rockland Immunochemicals, Gilbertsville, PA), at a dose of 30ug/g body weight on day 8 and day 11 after birth. The flow cytometry analyses were done at 3 weeks of age. For anti-IL7Rα antibody treatment, CTLA4RNAi/B6.H2^{g7} mice were intraperitoneally administered with anti-IL7Rα (A7R34) antibody or Rat IgG1 isotype control antibody (BioXcell, West Lebanon, NH) at a dose of 25ug/g body weight beginning at 3–4 days of age, twice a week for 3 weeks. These mice were then monitored for diabetes occurrence every 2–3 days till diabetes onset, or for 6 weeks. For anti-IFNγ antibody treatment, CTLA4RNAi/B6.H2^{g7} mice were intraperitoneally administered with anti-IFNγ (clone XMG1.2) antibody or Rat IgG isotype control antibody (BioXcell) at a dose of 25ug/g body weight beginning at 3–4 days of age, twice a week for 3 weeks. These mice were then monitored for diabetes occurrence every 2–3 days till diabetes onset, or for 6 weeks.

Statistics

Log-rank (Mantel-Cox) test was used for cumulative diabetes incidence. Student's *t* tests were used for single comparisons (Mean ± SEM). For the cells numbers in the pancreas of anti-CTLA4 treated BDC2.5/NOD mice, Mann Whitney U test was used to test for significance because of the high variability of cell numbers in the tissue of young mice.

$p<0.05$ was considered statistically significant. *$p<0.05$; **$p<0.01$; ***$p<0.005$; ns, not significant.

Results

Synergism between a modest reduction of CTLA4 expression and a permissive MHC locus was sufficient for the onset of autoimmune diabetes in mice at juvenile age

To analyze the impact of modest reductions in CTLA4 expression on T1D development in a context of the disease-susceptible *MHC* locus that contains $H2^{g7}$, without the influence of other T1D-risk loci, we crossed the CTLA4RNAi/B6 line (20, 21) with a commercially available congenic line, B6.NOD-(*D17Mit21-D17Mit10*) (22), which has the B6 genetic background harboring the *D17Mit21-D17Mit10* gene segment containing the $H2^{g7}$ *MHC* locus (hereto referred to as "B6.H2^{g7}"). This combination led to a line referred to as "CTLA4RNAi/B6.H2^{g7}". The CTLA4RNAi transgene causes a ~60% reduction in CTLA4 (19). When it was introduced into the B6.H2^{g7} genetic background, it resulted in diabetes onset in animals before reaching adulthood, which reflects human T1D onset at juvenile age. Diabetes onset was observed in 30% of these mice at 3–4 weeks of age. No diabetes was detected in the B6.H2^{g7} mice with normal CTLA4 levels (Fig. 1A). No gender bias in the occurrence of T1D was detected in this model (Fig. 1B). Therefore, this model recapitulated the features of juvenile-onset and lack of gender bias (30) in human T1D development with a natural immune cell repertoire. Histological analyses of pancreata from the non-diabetic CTLA4RNAi/B6.H2^{g7} mice showed increased islet infiltration in the pancreas (Fig. 1C–D). No lymphoproliferation was observed in CTLA4RNAi/B6.H2^{g7} mice, except in the pancreatic lymph nodes (PLN) where a 2–3 fold increase in cellularity was observed (Data not shown).

The induction of T1D in this model depended on the T1D-susceptible *MHC* locus since CTLA4RNAi on the wild type B6 background did not cause diabetes. However, there was increased pancreatic islet destruction in CTLA4RNAi/B6 mice from 10 weeks of age on when compared to wild-type B6 mice (Fig. 1E–F).

Diabetes incidence was not due to defective T_{reg} function; rather, a modest reduction in CTLA4 expression resulted in superior suppression by T_{reg} cells

The autoimmune damage to pancreatic islets induced by CTLA4 reduction could be due to defective regulation by T_{reg} cells. Previous studies have shown that specific loss of CTLA4 in T_{reg} cells leads to massive lymphoproliferative diseases due to their functional impairment (31). To assess if the function of T_{reg} cells is compromised by a modest reduction in CTLA4 levels, we performed *in vivo* and *in vitro* T_{reg} suppression experiments.

To test the suppressive ability of CTLA4RNAi T_{reg} cells *in vivo*, we used a standard model of T_{reg} cell reconstitution to neonate Foxp3-deficient B6 mice (32). We transferred naïve T_{reg} cells from CTLA4RNAi or control mice into the B6.$Foxp3^{sf}$ line (26) of Foxp3-deficient mice. Neonate $Foxp3^{sf}$ mice were reconstituted with naïve $CD4^+CD62L^+Foxp3^{FIR+}$ T_{reg} cells purified by flow cytometry from CTLA4RNAi or control B6 mice. Contrary to expectations, T_{reg} cells from CTLA4RNAi donors suppressed $CD4^+$

and $CD8^+$ T cell activation better than control T_{reg} cells (Fig. 2A–B). *Foxp3*^{sf} mice have characteristic inflammatory infiltration in the portal areas of the liver (33) which can be rectified by T_{reg} cell reconstitution (32). Indeed, fewer infiltrates were observed in the livers of Foxp3-deficient mice reconstituted with CTLA4RNAi T_{reg} cells when compared to those reconstituted with control T_{reg} cells, which was confirmed by histopathological analyses of these livers (Fig. 2C–D).

To further test the impact of a modest reduction in CTLA4 levels on T_{reg} cell function, an *in vitro* suppression assay was performed. A modest insufficiency of CTLA4 increased the suppressive ability of T_{reg} cells *in vitro*, with CTLA4RNAi T_{reg} cells exhibiting a significant increase in suppressive ability (Fig. 2E). Together these experiments suggest that a reduction in CTLA4 levels may enable T_{reg} cells to become better suppressors *in vivo* and *in vitro*.

Enhanced suppressive ability of T_{reg} cells was accompanied by an increased regulatory effector memory phenotype

Superior suppression mediated by T_{reg} cells with a reduction in CTLA4 levels could be attributed to the impact of CTLA4 reduction on their differention or activation. To explore this possibility, we analyzed the phenotype of the T_{reg} populations impacted by CTLA4RNAi in mice on the T1D-susceptible (B6.H2^{g7}) or -resistant (B6) backgrounds in the pancreas and the lymph nodes (Fig. 3A–C). Flow cytometry analyses showed that there was an increase in the total T_{reg} population in CTLA4RNAi mice on either the B6.H2^{g7} or the B6 background (data not shown). These T_{reg} cells were also phenotypically more memory-like, with a substantial increase in the total number of effector memory T_{reg} ($T_{reg\text{-}EM}$) cells in the target tissue (Fig. 3A–C). It has been recently shown that $T_{reg\text{-}EM}$ cells are able to confer superior protection in the tissue by being able to respond to autoimmune attack faster than effector T_{reg} ($T_{reg\text{-}EFF}$) cells (4). Thus, the increased number of $T_{reg\text{-}EM}$ cells in the pancreas of the CTLA4RNAi model would imply superior regulation by the T_{reg} cells at the site of ongoing autoimmunity.

A polyclonal T-cell repertoire system such as the CTLA4RNAi/B6.H2^{g7} and CTLA4RNAi/B6 models represent the natural T-cell repertoire in humans; however it is often difficult to pinpoint the response of antigen-specific cells. To study the effect of CTLA4RNAi on antigen-specific T_{reg} cells in autoimmune damage, we used the BDC2.5/NOD model, a well characterized MHC-class-II restricted TCR transgenic mouse model of T1D where the $CD4^+$ T cells specifically recognize a natural β-cell auto antigen (34).

Flow cytometry analyses of the pancreas of these mice revealed that a majority of the activated auto antigen-specific T_{reg} population was phenotypically effector memory like and the proportion of the $T_{reg\text{-}EM}$ population in the pancreas was 3-fold higher when compared to the draining lymph nodes (PLN) (Fig. 3D–E). On the other hand, the activated T_{reg} cells in the PLN were comprised primarily of $T_{reg\text{-}EFF}$ cells (Fig. 3D–E). T_{reg} cells in the pancreatic infiltrate of BDC2.5/NOD mice have been shown to be primarily responsible for suppressing tissue damage by the infiltrating autoimmune T_{conv} cells (28). Therefore, the increased proportion of antigen-specific $T_{reg\text{-}EM}$ cells in the pancreas of BDC2.5/NOD mice emphasizes the importance of this subset in conferring superior protection at the forefront of

autoimmune damage in the tissue. CTLA4 reduction further increased the antigen-specific $T_{reg\text{-}EM}$ population in the pancreas and pancreatic lymph nodes (Fig. 3F), suggesting enhanced T_{reg} regulation at the site of ongoing autoimmunity in a setting of reduced CTLA4 expression.

Thus a modest reduction in CTLA4 levels may lead to decreased intrinsic control of T_{reg} cells, resulting in their increased effector memory-like characteristics that potentiate their increased suppressive ability. This outcome is opposite to what was expected based on the effect of a complete ablation of CTLA4 in T_{reg} cells (31), suggesting that a modest reduction in CTLA4 levels, as detected in some human patients with an increased susceptibility to T1D, may lead to an effect on T_{reg} function opposite to that of complete blockade of CTLA4.

Predominance of $CD4^+$ effector memory cells in the T_{conv} compartment in the pancreas was associated with autoimmune diabetes

Previous studies have shown a complexity of CTLA4 function in regulating the T_{conv} compartment by both cell-extrinsic and cell-intrinsic mechanisms (35–37). Since the increased susceptibility to T1D by CTLA4RNAi in the B6.H2^{g7} background was not due to a defective T_{reg} compartment, we investigated the effects of CTLA4RNAi on the T_{conv} compartment.

To study the T_{conv} cell compartments including T_{CM}, T_{EM} and T_{EFF} cells, surface markers CD44, CD62L, CD69 and CD127 were used to analyze these subsets in the PLN and pancreas (Fig. 4A). Within the $CD8^+$ T cell compartment, there was little activation observed in the pancreatic lymph nodes (Fig. 4A). The percentage of $CD8^+$ T_{EM} cells in the pancreas was around 10% of the total $CD8^+$ population (Fig. 4A–B). However, there was no significant difference between CTLA4RNAi and control mice in this population. These two groups had no difference in the percentage of $CD8^+$ T_{EFF} (Fig. 4C) or $CD8^+$ T_{CM} (Fig. 4D) cells either.

Unlike the CD8 compartment, analyses of the CD4 compartment revealed a substantial increase in the $CD4^+$ T_{EM} cells in the pancreas of CTLA4RNAi mice versus controls (Fig. 5A–E). The highest proportion of $CD4^+$ T_{EM} cells was found in the pancreas (Fig. 5B, 5E), with a further ~2-fold increase in their proportion in the pancreas of CTLA4RNAi/B6.H2^{g7} mice compared to controls (Fig. 5B). This increase in proportion was also reflected as an increase in the total number of $CD4^+$ T_{EM} cells in the pancreas of CTLA4RNAi/B6.H2^{g7} mice (Fig. 5B). The increase in the autoimmune $CD4^+$ T_{EM} population in the pancreas of CTLA4RNAi mice was also accompanied by an increase in the total numbers of $CD4^+$ T_{EFF} cells in the target tissue (Fig. 5C). However, compared to the high percentage of the $CD4^+$ T_{EM} population (average 30%) in the $CD4^+$ T_{conv} compartment in the pancreas, the $CD4^+$ T_{EFF} population is only a minor subset (average 2%) in the tissue of CTLA4RNAi/B6.H2^{g7} mice. There was no difference observed in the $CD4^+$ T_{CM} compartment in the tissue of CTLA4RNAi/B6.H2^{g7} mice compared to the controls (Fig. 5D). Similar increases in the $CD4^+$ T_{EM} subset were detected in the pancreas of CTLA4RNAi/B6 mice (Fig. 5E).

T_{CM} cells are thought to reside in lymph nodes. We analyzed the T_{CM} compartment in the PLN, and found that there was an increase in the proportion of $CD4^+$ T_{CM} in the PLN of the CTLA4RNAi mice over controls (Fig. 5D). However, constant persistence of self-antigens may be untoward to the development of T_{CM} cells, akin to chronic infection settings (38). Thus it remains unknown whether this population of T cells with the central memory phenotype in the lymph nodes of CTLA4RNAi mice has a pathogenic potential.

Akin to CTLA4, PD-1 is another member of the CD28 family of receptors that has been shown to play an important role in T cell regulation and the dysregulation of which has been implicated in autoimmune diabetes (39–41). We analyzed PD-1 expression on the $CD4^+$ T_{EM} and $CD4^+$ T_{EFF} compartments in B6.H2^{g7} mice (Fig. 5F–G). A substantially greater proportion of $CD4^+$ T_{EFF} cells expressed PD-1 when compared to the $CD4^+$ T_{EM} cells (Fig. 5G). This implied that the autoimmune $CD4^+$ T_{EM} compartment could be more resistant than the $CD4^+$ T_{EFF} compartment to exhaustion meditated by the PD-1 pathway. A reduction in CTLA4 levels in B6.H2^{g7} mice, however, had no significant impact on PD-1 expression in the $CD4^+$ T_{EM} and $CD4^+$ T_{EFF} subsets (Fig. 5H).

CTLA4 reduction promoted auto antigen-specific $CD4^+$ T_{EM} in the T_{conv} compartment in target tissue

To characterize the memory phenotype of auto antigen-specific cells in the T_{conv} compartment, we used the BDC2.5/NOD model (34). The known antigen-specificity of the T cells against pancreatic β cells allows us to test the diabetogenic potential of the autoimmune $CD4^+$ T_{EM} and T_{EFF} cells. We purified the two subsets from BDC2.5/NOD.Foxp3^{FIR} spleens and adoptively transferred them into NOD.SCID mice. Indeed, the T_{EM} cells but not the T_{EFF} cells, caused diabetes efficiently (Fig. 6A), demonstrating that the $CD4^+$ T_{EM} compartment has a much higher pathogenic potential than the $CD4^+$ T_{EFF} compartment. Flow cytometry analyses revealed a comparable proportion of $CD4^+$ T cells in the NOD.SCID mice transferred with the $CD4^+$ T_{EM} or $CD4^+$ T_{EFF} cells, in the PLN (Fig. 6B) and other lymphoid organs (not shown), implying that the heightened autoimmune pathogenicity of $CD4^+$ T_{EM} cells over the $CD4^+$ T_{EFF} subset was not due to an advantage of expansion and/or survival of the $CD4^+$ T_{EM} subset over the $CD4^+$ T_{EFF} cells in the lymphopenic environment in NOD.SCID mice. To compare the auto antigen-specific responses of these subsets in a lymphoreplete system, the $CD4^+$ T_{EM} or the $CD4^+$ T_{EFF} subsets were purified from BDC2.5/NOD.Foxp3^{FIR} mice and were adoptively transferred into CD90.1 congenic NOD mice. Flow cytometry analyses revealed that an increased number of the transferred $CD4^+$ T_{EM} cells could be detected in the draining lymph nodes of the recipient mice when compared to that in the animals transferred with $CD4^+$ T_{EFF} cells (Supplemental Fig. 1).

To study the effect of reduced levels of CTLA4 on this pathogenic $CD4^+$ T_{EM} compartment, we generated CTLA4RNAi/BDC2.5 mice or PL4/BDC2.5 controls by crossing the CTLA4RNAi/NOD model or the PL4/NOD line with the BDC2.5/NOD line. The 60% reduction in CTLA4 levels resulted in 100% of the mice becoming diabetic by 12–16 weeks of age, whereas no diabetes was detected up to this age in the CTLA4RNAi-transgene-negative BDC2.5 or PL4/BDC2.5 control groups (Fig. 6C). This corresponded with an

average 7-fold increase in the total number of auto antigen-specific $CD4^+$ T_{EM} in the pancreas (Fig. 6D–E), similar to the CTLA4RNAi/B6.H2^{g7} (Fig. 5B) and CTLA4RNAi/B6 (Fig. 5E) models. This increase in the $CD4^+$ T_{EM} compartment by CTLA4RNAi was apparently antigen-driven, as it was observed only in the tissue (pancreas) and the draining lymph nodes (PLN) but not in the non-draining inguinal lymph nodes (ILN) (Fig. 6E). It was interesting to note that there was no effect of a reduction in CTLA4 levels on the percentage of auto antigen-specific $CD4^+$ T_{EFF} cells in this model (Fig. 6F). The increased total number of $CD4^+$ T_{EFF} cells in the PLN (Fig. 6F) was due to increased cellularity in the PLN of the CTLA4RNAi model. This data reinforces the idea that the $CD4^+$ T_{EM} rather than the $CD4^+$ T_{EFF} compartment plays a key role in T1D pathogenesis. Furthermore, the effect of CTLA4 modulation on the T_{EM} compartment was also evident with anti-CTLA4 antibody blockade (Supplemental Fig. 2).

Increased production of IL17 and IFNγ by the pathogenic autoimmune $CD4^+$ T_{EM} compartment due to a reduction in CTLA4 levels

Persistence of antigens in chronic infectious diseases has been shown to result in exhausted T cells that produced reduced levels of cytokines. However, despite persistence of self-antigens in the context of autoimmune diseases, the production of IL17 and IFNγ by T cells has been implicated in the pathogenesis of various autoimmune diseases including T1D (42).

To characterize the production of pathogenic cytokines by the autoimmune T_{EFF} and T_{EM} compartments during T1D development, T_{EFF} and T_{EM} subsets were analyzed for their cytokine production in the pancreas and PLNs of BDC2.5/NOD mice (Fig. 7A). Analyses using intracellular flow cytometry showed that T_{EM} cells were the predominant producers of IL17 in both the PLN and in the pancreas (Fig. 7A–B). On the other hand both the T_{EFF} and the T_{EM} subsets produced IFNγ, with a greater proportion of the PLN T_{EM} subset producing IFNγ when compared to the PLN T_{EFF} subset (Fig. 7B). Clearly, compared to the IFNγ and IL17 production in the PLN, the production of these cytokines by the auto antigen-specific $CD4^+$ T_{EM} cells was not impeded in the pancreas despite persistence of self-antigens in the target tissue (Fig. 7A–B).

We further analyzed the impact of CTLA4 modulation on cytokine production by the autoimmune $CD4^+$ T_{EM} and $CD4^+$ T_{EFF} cells in the PLN and pancreas (Fig. 7C–H). Intracellular cytokine staining revealed a 2-fold increase in the total number of IL17-producing $CD4^+$ T_{EM} cells in the pancreas of CTLA4RNAi mice compared to controls (Fig. 7C). CTLA4 reduction also led to a 3-fold increase in the total number of IFNγ-producing autoimmune $CD4^+$ T_{EM} cells (Fig. 7E) and a 2-fold increase in the IFNγ-producing autoimmune $CD4^+$ T_{EFF} cells in the pancreas (Fig. 7G). The impact of CTLA4RNAi on Th1 and Th17 memory was similar to that of CTLA4 blockade by monoclonal antibody treatments. Anti-CTLA4 treatment in young BDC2.5/NOD mice resulted in an increase in the total number of Th17 T_{EM} (Fig. 7D) and Th1 T_{EM} (Fig. 7F) cells in the PLN and pancreas.

Anti-IL7Rα treatment reduced Th17 memory in the tissue but without substantial effect on T1D development

On the B6.H2^{g7} background, a reduction in CTLA4 levels led to a 3-fold increase in the percentage of IL17-producing CD4$^+$ cells (Fig. 8A–B) and a 2-fold increase in the percentage of IFNγ-producing CD4$^+$ T cells (Fig. 8C) in the draining lymph nodes (PLN). This amounted to a 7-fold increase in the total numbers of IL17-producing CD4$^+$ T cells (Fig. 8B) and a 4-fold increase in the total numbers of IFNγ-producing CD4$^+$ T cells (Fig. 8C) in CTLA4RNAi/B6.H2^{g7} mice compared to the controls.

Given the prominent role of IL7 in T cell memory development (43, 44), we used monoclonal antibodies against IL7-receptor α (IL7Rα, CD127) to inhibit diabetes development in the juvenile-onset T1D model. We treated CTLA4RNAi/B6.H2^{g7} mice with anti-IL7Rα antibody for 3 weeks after birth. The treatment efficiently blocked IL7Rα (Supplemental Fig. 3). However, there was no significant decrease in diabetes incidence on anti-IL7Rα treatment when compared to the isotype control treatment (Fig. 8D). In the anti-IL7Rα treated group, 37% of CTLA4RNAi/B6.H2^{g7} mice became diabetic at 21–26 days of age which is similar to the 30% diabetes incidence in untreated CTLA4RNAi/B6.H2^{g7} mice as shown in Fig. 1A. However, there was a ~3-fold decrease in the proportion of IL17-producing CD4$^+$ T cells in the pancreas and draining lymph nodes (Fig. 8E–F). This effect was sustained for 5–6 weeks after the last treatment. On the other hand, there was no significant reduction in the proportion of IFNγ- producing CD4$^+$ T cells in the pancreas of anti-IL7Rα antibody treated mice (Fig. 8E–G). The reduction in total numbers of IFNγ-producing cells in the lymph nodes (Fig. 8G) could be attributed to the overall reduction in total T cell numbers caused by the anti-IL7Rα treatment, as has been shown in other studies as well (23, 24). The reduction in the percentage of the Th17 subset but not that of the Th1 subset suggests a different mechanism of action of anti-IL7Rα antibody treatment in the juvenile-onset T1D model when compared to adulthood-onset diabetes observed in the standard NOD model (23, 24). Our data also suggests that IL17 may not play a major role in this setting of juvenile-onset diabetes.

To further examine whether IFNγ plays a role in autoimmune pathogenicity caused by reduced levels of CTLA4, we used anti-IFNγ antibody treatment. IFNγ blockade curtailed diabetes development in CTLA4RNAi/B6.H2^{g7} mice. The treatment suppressed but did not abrogate insulitis in the animals (Fig. 9A–B), nor did it decrease the population size of the CD4$^+$ T_{EM} subset (data not shown). We then examined the role of Th17 by using a line of IL17A-deficient mice available on the B6 genetic background. As shown in Fig. 1E–F, CTLA4 reduction caused insulitis development in B6 mice although diabetes was not observed. Absence of IL17A in CTLA4RNAi/B6.IL17$^-$ mice did not reduce the pancreatic islet infiltration caused by a reduction in CTLA4 (Fig. 9C–D), nor did it alter the percentage and number of T_{EM} cells in the draining lymph nodes (Fig. 9E–F). These results are consistent with the observation that a reduction in the Th17 subset did not lead to a decrease in diabetes development in the CTLA4RNAi/B6.H2^{g7} mice treated with IL-7Rα blockade (Fig. 8E–F). Overall, our observations with regard to the Th1 versus the Th17 subsets in autoimmune damage of the pancreatic islets caused by CTLA4 reduction are consistent with

the well-recognized pathogenicity of Th1 cells but a debated role of the Th17 subset in autoimmune diabetes (27, 45).

Discussion

Immunological memory is thought to perpetuate chronic damage in autoimmune diseases. Memory cell formation is influenced by a number of peripheral immune regulatory genes, among which *CTLA4* levels have long been associated with various autoimmune diseases including T1D (8). It has been shown that CTLA4 blockade increased the population of $CD8^+$ $CD44^{hi}CD62L^{lo}$ T cells, suggesting a role of CTLA4 in $CD8^+$ T cell memory in a model of acute infection (46). However, studies in other acute infection models have shown that CTLA4 does not play an important role in memory formation, but rather plays a T_{reg}-mediated role in their quality with respect to cytokine production (47). In our study, we analyzed how a modest variation in CTLA4 levels affects subsets of effector and memory T cells in autoimmune diabetes settings. Multiparametric flow cytometry analyses of the autoimmune models clearly identified T_{EM} cells from short-lived T_{EFF} cells, both of which are present in the $CD44^{hi}CD62L^{lo}$ pool, with consistent cytokine profiles in *ex vivo* analyses, and pathogenic potency *in vivo* as revealed by transfer of autoimmune diabetes.

The novel CTLA4RNAi/B6.H2^{g7} model recapitulates key aspects of human T1D: onset at juvenile age, natural T-cell repertoire and no gender bias. It offered us an opportunity to examine memory and effector T cell subsets in young animals and to study the effect of a reduction in CTLA4 levels in conjunction with a disease-susceptible *MHC*. This system also closely resembled human T1D where some disease-susceptible polymorphisms result in lower levels of CTLA4 expression (9–11) and are associated with T1D risk. We also show that while a disease-susceptible *MHC* is required for progression to frank diabetes onset, a reduction in CTLA4 levels is sufficient to elicit lymphocytic islet infiltration even in a disease-resistant genetic background, as shown in the CTLA4RNAi/B6 model.

In the NOD model, there was an increase of islet-specific glucose-6-phosphatase catalytic subunit related protein (IGRP)-specific $CD8^+$ T_{EM} cells in the peripheral lymphoid tissue (spleen and peripheral lymph nodes) after 10 weeks of age, which correlated with severity of insulitis in these mice (48). In our CTLA4RNAi/B6.H2^{g7} model of juvenile-onset T1D that harbors a natural polyclonal T-cell repertoire as in the NOD model, we did not detect substantial impact of $CD8^+$ memory T cells on the early onset of autoimmune diabetes. However, we found that the increased presence of $CD4^+$ T_{EM} cells in the pancreatic tissue, the site of ongoing autoimmune destruction, correlates with juvenile-onset disease incidence in CTLA4RNAi/B6.H2^{g7} mice. Although there was also an increase in the total number of short-lived $CD4^+$ T_{EFF} cells in the pancreas in this model, the proportion of the $CD4^+$ T_{EFF} compartment (average 2%) was minor compared to the $CD4^+$ T_{EM} subset (average 30%) in the tissue. Additionally, our adoptive transfer studies using an auto antigen-specific BDC2.5/NOD model revealed that the $CD4^+$ T_{EM} subset was likely much more potent in eliciting the autoimmune disease. These autoimmune $CD4^+$ T_{EM} cells were also potent producers of pathogenic cytokines like IFNγ and IL17 with the IL17 being produced only within the $CD4^+$ T_{EM} compartment. This is in contrast to an acute infection model where only short lived $CD4^+$ T_{EFF} cells produce IL17 (49) and supports the notion of autoimmune

Th17 memory as has been recently shown (50). Unlike in chronic infections and a model of skin autoimmune disease, where persistence of antigens impairs cytokine production in the target tissue (5, 51), these autoimmune $CD4^+$ T_{EM} cells produced as much IL17 and IFNγ in the pancreas as they did in the draining lymph nodes.

Interestingly, a reduction in CTLA4 expression in T_{reg} cells promoted their suppressive ability. A previous study showed that complete deficiency of CTLA4 in T_{reg} cells impaired their suppressive ability despite increased proliferation and activation of these T_{reg} cells (31). This apparent disparity could be explained by sufficient levels of CTLA4 that are available to the T_{reg} cells for them to function as suppressors when CTLA4 levels are only reduced and not completely ablated. These CTLA4RNAi T_{reg} cells however exhibited increased suppressive ability because of their increased effector memory formation likely due to reduced regulation by CTLA4. Indeed, regulatory memory T cells at the target tissue are thought to play a crucial role in preventing an autoimmune response (52). While some studies have shown that T_{reg} cells in T1D patients are functionally impaired (53, 54), others have suggested that these T_{reg} cells can still function as potent suppressors (55). Our results suggest that the specific genetic risk factors that predispose some patients to T1D may influence T_{reg} cell functional status depending on the quantitative variations in gene expression. Thus in patients with CTLA4 insufficiency, their natural T_{reg} cells could have a superior potential to suppress autoimmune responses. Therefore, targeting the patient's own T_{reg} expansion may offer greater therapeutic potential. Of note, our results indicate that modest reduction of CTLA4 enhanced not only the formation but also the function of T_{reg} memory, suggesting a possible role of CTLA4 in the exhaustion of T_{reg} memory, unlike in the $CD8^+$ T_{EFF} counterpart (56). This finding also opens up the possibilities for adoptive T_{reg} therapy, where expansion of T_{reg} cells *in vitro* could be supplemented by a reduction in CTLA4 brought about by CTLA4RNAi, thus increasing their expansion, suppression and memory potentials in not only autoimmune diseases but also in transplantation settings. These engineered memory T_{reg} cells would also offer the prospect of a long-lived compartment that has the potential to protect in the long-term.

Recent studies have shown a predominant effect of cell-extrinsic regulation by CTLA4, in T_{reg} cells, on antigen-presenting cells (31). The superior suppressive ability of CTLA4RNAi T_{reg} cells, although not necessarily contradicting that concept, suggests the importance of CTLA4 regulation in T_{reg} cells, particularly in their differentiation to potent $T_{reg\text{-}EM}$ cells. In the T_{conv} compartment, the critical role of $CD4^+$ T_{EM} cells in autoimmune diseases suggests an important therapeutic target. Given the function of IL7 in memory cell formation, a major initiative is being undertaken to develop therapeutic interventions by blocking IL7 signaling. The treatment has indeed shown success in the standard NOD model of autoimmune diabetes (23, 24). In an EAE model, blocking IL7 signaling led to reduction in the Th17 population (57). In our CTLA4RNAi model, even though anti-IL7Rα treatment inhibited differentiation of the Th17 subset, it did not suppress autoimmune Th1 differentiation, and did not inhibit the juvenile-onset of T1D. A potential role of Th1 effector memory cells appears consistent with a previous study with mouse model of EAE (58). Therefore, it is possible that failure of the anti-IL7Rα treatment in curtailing Th1 formation in the young animals may account for the failure of the treatment in suppressing T1D in our model.

Indeed, blocking IFNγ with antibody treatment suppressed diabetes development in the CTLA4RNAi/B6.H2^{g7} model of juvenile-onset T1D caused by CTLA4 reduction in a natural T-cell repertoire. Of note, a fully humanized monoclonal antibody against IFNγ has been under clinical trials (ClinicalTrials.gov). Therefore it is possible in the relatively near future to learn whether anti-IFNγ treatment can suppress juvenile-onset T1D in human beings.

In conclusion, this study of an early-onset model of T1D with a natural T-cell repertoire illustrates the apparently opposing effects of CTLA4 insufficiency, in enhancing protection by T_{reg} cells but increasing the pathogenicity of the CD4$^+$ T_{conv} cells. These dichotomized effects converged at the increased effector memory formation in both T_{reg} and T_{conv} compartments. While suppressing memory formation in the T_{conv} compartment may be desirable in the therapeutic development against autoimmune diseases, promoting the formation of memory T_{reg} cells, especially $T_{reg\text{-}EM}$, could be used to control autoimmune damage. Therefore, although T_{reg} cells depend on the presence of CTLA4 for functionality (31), a subtle reduction of CTLA4 levels in T_{reg} cells could be engineered to promote $T_{reg\text{-}EM}$ formation and thus to promote efficacies of T_{reg} adoptive cell therapies.

Supplementary Material

Refer to Web version on PubMed Central for supplementary material.

Acknowledgments

We thank Dr. H. Dooms for the anti-IL7Rα hybridoma clone A7R34, Dr. O. Umland for his expert flow cytometry advice, Mr. J. Enten, Dr. S. Opiela and Mrs. Patricia Guevara for their cell sorting assistance and Mr. K. Johnson for his assistance with histology.

Source of support: This work was supported by grants from the National Institutes of Health (DP3DK085696 to ZC). The content is solely the responsibility of the authors and does not necessarily represent the official views of the NIDDK or NIH.

Abbreviations used in manuscript

T1D	Type 1 Diabetes
RNAi	RNA interference
RFP	Red Fluorescent Protein
FIR	Foxp3-IRES-RFP
CPM	Counts Per Minute
T_{reg}	Regulatory T cells
T_{conv}	Conventional T cells
$T_{reg\text{-}EFF}$	Regulatory Effector T cells
$T_{reg\text{-}EM}$	Regulatory Effector Memory T cells
T_{EM}	Conventional Effector memory T cells

T_{EFF}	Conventional Effector T cells
T_{CM}	Conventional Central Memory T cells
PLN	Pancreatic Lymph Node
ILN	Inguinal Lymph Node
UTR	Untranslated Region
SNP	Single Nucleotide Polymorphism
IGRP	Islet specific Glucose-6-phosphatase catalytic subunit Related Protein
EAE	Experimental Autoimmune Encephalomyelitis

References

1. Devarajan P, Chen Z. Autoimmune effector memory T cells: the bad and the good. Immunol Res. 2013; 57:12–22. [PubMed: 24203440]
2. Brincks EL, Roberts AD, Cookenham T, Sell S, Kohlmeier JE, Blackman MA, Woodland DL. Antigen-specific memory regulatory CD4+Foxp3+ T cells control memory responses to influenza virus infection. J Immunol. 2013; 190:3438–3446. [PubMed: 23467933]
3. Sanchez AM, Zhu J, Huang X, Yang Y. The development and function of memory regulatory T cells after acute viral infections. J Immunol. 2012; 189:2805–2814. [PubMed: 22855712]
4. Rosenblum MD, Gratz IK, Paw JS, Lee K, Marshak-Rothstein A, Abbas AK. Response to self antigen imprints regulatory memory in tissues. Nature. 2011; 480:538–542. [PubMed: 22121024]
5. Gratz IK, Rosenblum MD, Maurano MM, Paw JS, Truong HA, Marshak-Rothstein A, Abbas AK. Cutting Edge: Self-Antigen Controls the Balance between Effector and Regulatory T Cells in Peripheral Tissues. J Immunol. 2014; 192:1351–1355. [PubMed: 24442443]
6. Pociot F, McDermott MF. Genetics of type 1 diabetes mellitus. Genes Immun. 2002; 3:235–249. [PubMed: 12140742]
7. Teft WA, Kirchhof MG, Madrenas J. A molecular perspective of CTLA-4 function. Annu Rev Immunol. 2006; 24:65–97. [PubMed: 16551244]
8. Kristiansen OP, Larsen ZM, Pociot F. CTLA-4 in autoimmune diseases--a general susceptibility gene to autoimmunity? Genes Immun. 2000; 1:170–184. [PubMed: 11196709]
9. Ligers A, Teleshova N, Masterman T, Huang WX, Hillert J. CTLA-4 gene expression is influenced by promoter and exon 1 polymorphisms. Genes Immun. 2001; 2:145–152. [PubMed: 11426323]
10. Wang XB, Zhao X, Giscombe R, Lefvert AK. A CTLA-4 gene polymorphism at position −318 in the promoter region affects the expression of protein. Genes Immun. 2002; 3:233–234. [PubMed: 12058260]
11. Anjos S, Nguyen A, Ounissi-Benkalha H, Tessier MC, Polychronakos C. A common autoimmunity predisposing signal peptide variant of the cytotoxic T-lymphocyte antigen 4 results in inefficient glycosylation of the susceptibility allele. J Biol Chem. 2002; 277:46478–46486. [PubMed: 12244107]
12. Baniasadi V, Narain N, Goswami R, Das SN. Promoter region −318 C/ T and −1661 A/G CTLA-4 single nucleotide polymorphisms and type 1 diabetes in North Indians. Tissue Antigens. 2006; 67:383–389. [PubMed: 16671945]
13. Ueda H, Howson JM, Esposito L, Heward J, Snook H, Chamberlain G, Rainbow DB, Hunter KM, Smith AN, Di Genova G, Herr MH, Dahlman I, Payne F, Smyth D, Lowe C, Twells RC, Howlett S, Healy B, Nutland S, Rance HE, Everett V, Smink LJ, Lam AC, Cordell HJ, Walker NM, Bordin C, Hulme J, Motzo C, Cucca F, Hess JF, Metzker ML, Rogers J, Gregory S, Allahabadia A, Nithiyananthan R, Tuomilehto-Wolf E, Tuomilehto J, Bingley P, Gillespie KM, Undlien DE, Ronningen KS, Guja C, Ionescu-Tirgoviste C, Savage DA, Maxwell AP, Carson DJ, Patterson CC, Franklyn JA, Clayton DG, Peterson LB, Wicker LS, Todd JA, Gough SC. Association of the T-

cell regulatory gene CTLA4 with susceptibility to autoimmune disease. Nature. 2003; 423:506–511. [PubMed: 12724780]

14. Vijayakrishnan L, Slavik JM, Illes Z, Greenwald RJ, Rainbow D, Greve B, Peterson LB, Hafler DA, Freeman GJ, Sharpe AH, Wicker LS, Kuchroo VK. An autoimmune disease-associated CTLA-4 splice variant lacking the B7 binding domain signals negatively in T cells. Immunity. 2004; 20:563–575. [PubMed: 15142525]
15. Liu SM, Sutherland AP, Zhang Z, Rainbow DB, Quintana FJ, Paterson AM, Sharpe AH, Oukka M, Wicker LS, Kuchroo VK. Overexpression of the Ctla-4 isoform lacking exons 2 and 3 causes autoimmunity. J Immunol. 2012; 188:155–162. [PubMed: 22124121]
16. Gerold KD, Zheng P, Rainbow DB, Zernecke A, Wicker LS, Kissler S. The soluble CTLA-4 splice variant protects from type 1 diabetes and potentiates regulatory T-cell function. Diabetes. 2011; 60:1955–1963. [PubMed: 21602513]
17. Stumpf M, Zhou X, Bluestone JA. The B7-independent isoform of CTLA-4 functions to regulate autoimmune diabetes. J Immunol. 2013; 190:961–969. [PubMed: 23293354]
18. Anjos SM, Shao W, Marchand L, Polychronakos C. Allelic effects on gene regulation at the autoimmunity-predisposing CTLA4 locus: a re-evaluation of the 3' +6230G>A polymorphism. Genes Immun. 2005; 6:305–311. [PubMed: 15858600]
19. Chen Z, Stockton J, Mathis D, Benoist C. Modeling CTLA4-linked autoimmunity with RNA interference in mice. Proc Natl Acad Sci U S A. 2006; 103:16400–16405. [PubMed: 17060611]
20. Miska J, Bas E, Devarajan P, Chen Z. Autoimmunity-mediated antitumor immunity: tumor as an immunoprivileged self. Eur J Immunol. 2012; 42:2584–2596. [PubMed: 22777737]
21. Miska J, Abdulreda MH, Devarajan P, Lui JB, Suzuki J, Pileggi A, Berggren PO, Chen Z. Real-time immune cell interactions in target tissue during autoimmune-induced damage and graft tolerance. J. Exp. Med. 2014; 211:441–456. [PubMed: 24567447]
22. Yui MA, Muralidharan K, Moreno-Altamirano B, Perrin G, Chestnut K, Wakeland EK. Production of congenic mouse strains carrying NOD-derived diabetogenic genetic intervals: an approach for the genetic dissection of complex traits. Mamm Genome. 1996; 7:331–334. [PubMed: 8661724]
23. Penaranda C, Kuswanto W, Hofmann J, Kenefeck R, Narendran P, Walker LS, Bluestone JA, Abbas AK, Dooms H. IL-7 receptor blockade reverses autoimmune diabetes by promoting inhibition of effector/memory T cells. Proc Natl Acad Sci U S A. 2012; 109:12668–12673. [PubMed: 22733744]
24. Lee LF, Logronio K, Tu GH, Zhai W, Ni I, Mei L, Dilley J, Yu J, Rajpal A, Brown C, Appah C, Chin SM, Han B, Affolter T, Lin JC. Anti-IL-7 receptor-alpha reverses established type 1 diabetes in nonobese diabetic mice by modulating effector T-cell function. Proc Natl Acad Sci U S A. 2012; 109:12674–12679. [PubMed: 22733769]
25. Wan YY, Flavell RA. Identifying Foxp3-expressing suppressor T cells with a bicistronic reporter. Proc Natl Acad Sci U S A. 2005; 102:5126–5131. [PubMed: 15795373]
26. Brunkow ME, Jeffery EW, Hjerrild KA, Paeper B, Clark LB, Yasayko SA, Wilkinson JE, Galas D, Ziegler SF, Ramsdell F. Disruption of a new forkhead/winged-helix protein, scurfin, results in the fatal lymphoproliferative disorder of the scurfy mouse. Nat Genet. 2001; 27:68–73. [PubMed: 11138001]
27. Katz JD, Benoist C, Mathis D. T helper cell subsets in insulin-dependent diabetes. Science. 1995; 268:1185–1188. [PubMed: 7761837]
28. Chen Z, Herman AE, Matos M, Mathis D, Benoist C. Where CD4+CD25+ T reg cells impinge on autoimmune diabetes. J Exp Med. 2005; 202:1387–1397. [PubMed: 16301745]
29. Hirota K, Duarte JH, Veldhoen M, Hornsby E, Li Y, Cua DJ, Ahlfors H, Wilhelm C, Tolaini M, Menzel U, Garefalaki A, Potocnik AJ, Stockinger B. Fate mapping of IL-17-producing T cells in inflammatory responses. Nat Immunol. 2011; 12:255–263. [PubMed: 21278737]
30. Gale EA, Gillespie KM. Diabetes and gender. Diabetologia. 2001; 44:3–15. [PubMed: 11206408]
31. Wing K, Onishi Y, Prieto-Martin P, Yamaguchi T, Miyara M, Fehervari Z, Nomura T, Sakaguchi S. CTLA-4 control over Foxp3+ regulatory T cell function. Science. 2008; 322:271–275. [PubMed: 18845758]
32. Fontenot JD, Gavin MA, Rudensky AY. Foxp3 programs the development and function of CD4+CD25+ regulatory T cells. Nat Immunol. 2003; 4:330–336. [PubMed: 12612578]

33. Godfrey VL, Wilkinson JE, Russell LB. X-linked lymphoreticular disease in the scurfy (sf) mutant mouse. Am J Pathol. 1991; 138:1379–1387. [PubMed: 2053595]
34. Katz JD, Wang B, Haskins K, Benoist C, Mathis D. Following a diabetogenic T cell from genesis through pathogenesis. Cell. 1993; 74:1089–1100. [PubMed: 8402882]
35. Ise W, Kohyama M, Nutsch KM, Lee HM, Suri A, Unanue ER, Murphy TL, Murphy KM. CTLA-4 suppresses the pathogenicity of self antigen-specific T cells by cell-intrinsic and cell-extrinsic mechanisms. Nat Immunol. 2010; 11:129–135. [PubMed: 20037585]
36. Corse E, Allison JP. Cutting edge: CTLA-4 on effector T cells inhibits in trans. J Immunol. 2012; 189:1123–1127. [PubMed: 22753941]
37. Wang CJ, Kenefeck R, Wardzinski L, Attridge K, Manzotti C, Schmidt EM, Qureshi OS, Sansom DM, Walker LS. Cutting edge: cell-extrinsic immune regulation by CTLA-4 expressed on conventional T cells. J Immunol. 2012; 189:1118–1122. [PubMed: 22753931]
38. Wherry EJ, Barber DL, Kaech SM, Blattman JN, Ahmed R. Antigen-independent memory CD8 T cells do not develop during chronic viral infection. Proc Natl Acad Sci U S A. 2004; 101:16004–16009. [PubMed: 15505208]
39. Ansari MJ, Salama AD, Chitnis T, Smith RN, Yagita H, Akiba H, Yamazaki T, Azuma M, Iwai H, Khoury SJ, Auchincloss H Jr, Sayegh MH. The programmed death-1 (PD-1) pathway regulates autoimmune diabetes in nonobese diabetic (NOD) mice. J Exp Med. 2003; 198:63–69. [PubMed: 12847137]
40. Keir ME, Liang SC, Guleria I, Latchman YE, Qipo A, Albacker LA, Koulmanda M, Freeman GJ, Sayegh MH, Sharpe AH. Tissue expression of PD-L1 mediates peripheral T cell tolerance. J Exp Med. 2006; 203:883–895. [PubMed: 16606670]
41. Pauken KE, Jenkins MK, Azuma M, Fife BT. PD-1, but not PD-L1, expressed by islet-reactive CD4+ T cells suppresses infiltration of the pancreas during type 1 diabetes. Diabetes. 2013; 62:2859–2869. [PubMed: 23545706]
42. Bending D, Zaccone P, Cooke A. Inflammation and type one diabetes. Int Immunol. 2012; 24:339–346. [PubMed: 22447815]
43. Li J, Huston G, Swain SL. IL-7 promotes the transition of CD4 effectors to persistent memory cells. J Exp Med. 2003; 198:1807–1815. [PubMed: 14676295]
44. Kondrack RM, Harbertson J, Tan JT, McBreen ME, Surh CD, Bradley LM. Interleukin 7 regulates the survival and generation of memory CD4 cells. J Exp Med. 2003; 198:1797–1806. [PubMed: 14662907]
45. Emamaullee JA, Davis J, Merani S, Toso C, Elliott JF, Thiesen A, Shapiro AM. Inhibition of Th17 cells regulates autoimmune diabetes in NOD mice. Diabetes. 2009; 58:1302–1311. [PubMed: 19289457]
46. Pedicord VA, Montalvo W, Leiner IM, Allison JP. Single dose of anti-CTLA-4 enhances CD8+ T-cell memory formation, function, and maintenance. Proc Natl Acad Sci U S A. 2011; 108:266–271. [PubMed: 21173239]
47. Rudolph M, Hebel K, Miyamura Y, Maverakis E, Brunner-Weinzierl MC. Blockade of CTLA-4 decreases the generation of multifunctional memory CD4+ T cells in vivo. J Immunol. 2011; 186:5580–5589. [PubMed: 21478403]
48. Chee J, Ko HJ, Skowera A, Jhala G, Catterall T, Graham KL, Sutherland RM, Thomas HE, Lew AM, Peakman M, Kay TW, Krishnamurthy B. Effector-memory T cells develop in islets and report islet pathology in type 1 diabetes. J Immunol. 2014; 192:572–580. [PubMed: 24337380]
49. Pepper M, Linehan JL, Pagan AJ, Zell T, Dileepan T, Cleary PP, Jenkins MK. Different routes of bacterial infection induce long-lived TH1 memory cells and short-lived TH17 cells. Nat Immunol. 2010; 11:83–89. [PubMed: 19935657]
50. Haines CJ, Chen Y, Blumenschein WM, Jain R, Chang C, Joyce-Shaikh B, Porth K, Boniface K, Mattson J, Basham B, Anderton SM, McClanahan TK, Sadekova S, Cua DJ, McGeachy MJ. Autoimmune memory T helper 17 cell function and expansion are dependent on interleukin-23. Cell Rep. 2013; 3:1378–1388. [PubMed: 23623497]
51. Wherry EJ, Ahmed R. Memory CD8 T-cell differentiation during viral infection. J Virol. 2004; 78:5535–5545. [PubMed: 15140950]

52. Burzyn D, Benoist C, Mathis D. Regulatory T cells in nonlymphoid tissues. Nat Immunol. 2013; 14:1007–1013. [PubMed: 24048122]

53. Lindley S, Dayan CM, Bishop A, Roep BO, Peakman M, Tree TI. Defective suppressor function in CD4(+)CD25(+) T-cells from patients with type 1 diabetes. Diabetes. 2005; 54:92–99. [PubMed: 15616015]

54. Brusko TM, Wasserfall CH, Clare-Salzler MJ, Schatz DA, Atkinson MA. Functional defects and the influence of age on the frequency of CD4+ CD25+ T-cells in type 1 diabetes. Diabetes. 2005; 54:1407–1414. [PubMed: 15855327]

55. Putnam AL, Vendrame F, Dotta F, Gottlieb PA. CD4+CD25high regulatory T cells in human autoimmune diabetes. J Autoimmun. 2005; 24:55–62. [PubMed: 15725577]

56. Barber DL, Wherry EJ, Masopust D, Zhu B, Allison JP, Sharpe AH, Freeman GJ, Ahmed R. Restoring function in exhausted CD8 T cells during chronic viral infection. Nature. 2006; 439:682–687. [PubMed: 16382236]

57. Ashbaugh JJ, Brambilla R, Karmally SA, Cabello C, Malek TR, Bethea JR. IL7Ralpha contributes to experimental autoimmune encephalomyelitis through altered T cell responses and nonhematopoietic cell lineages. J Immunol. 2013; 190:4525–4534. [PubMed: 23530149]

58. Lee LF, Axtell R, Tu GH, Logronio K, Dilley J, Yu J, Rickert M, Han B, Evering W, Walker MG, Shi J, de Jong BA, Killestein J, Polman CH, Steinman L, Lin JC. IL-7 promotes T(H)1 development and serum IL-7 predicts clinical response to interferon-beta in multiple sclerosis. Sci Transl Med. 2011; 3 93ra68.

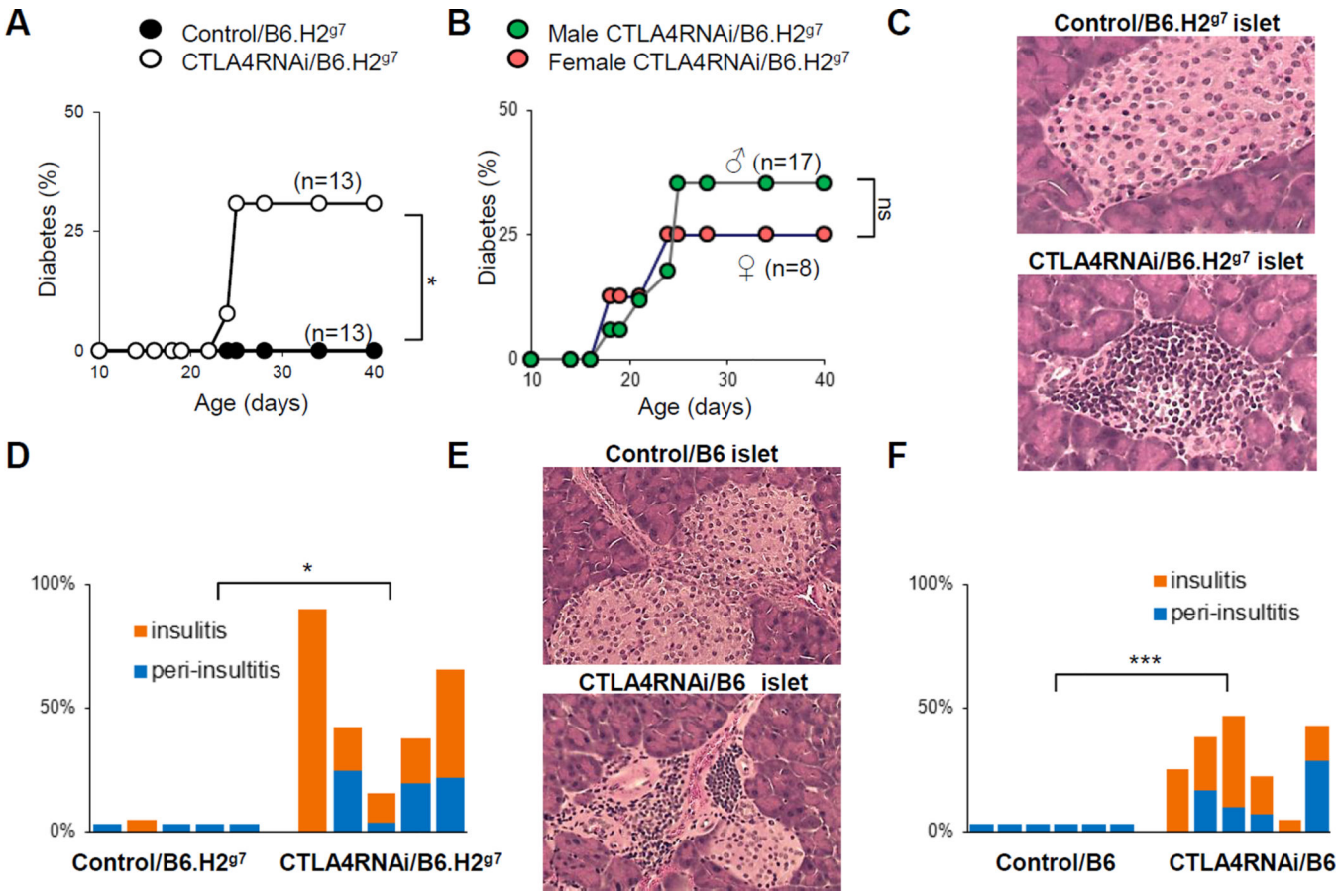

FIGURE 1. Modest reduction in CTLA4 accompanied by a permissive *MHC* locus was sufficient to induce T1D in mice at juvenile age

(**A**) CTLA4RNAi mice on the B6.H2^{g7} background and transgene-negative B6.H2^{g7} littermate controls were monitored for diabetes for 60 days. (**B**) Diabetes incidence in juvenile male and female CTLA4RNAi/B6.H2^{g7} mice. (**C**) Representative H&E sections of the pancreas from 19 day old mice (original magnification: x12.5). (**D**) Summary of islet infiltration in CTLA4RNAi/B6.H2^{g7} or transgene-negative B6.H2^{g7} littermate controls (n=5 per group). (**E**) Representative H&E sections of the pancreas from sex-matched 12–13 week old CTLA4RNAi or PL4 vector control mice on the diabetes-resistant B6 background (original magnification: x12.5). (**F**) Summary of islet infiltration in 10–27 week old CTLA4RNAi/B6 or PL4 vector control mice (age- and sex-matched, n=6 per group). Each bar represents one animal. *p<0.05; ***p<0.005; ns, not significant.

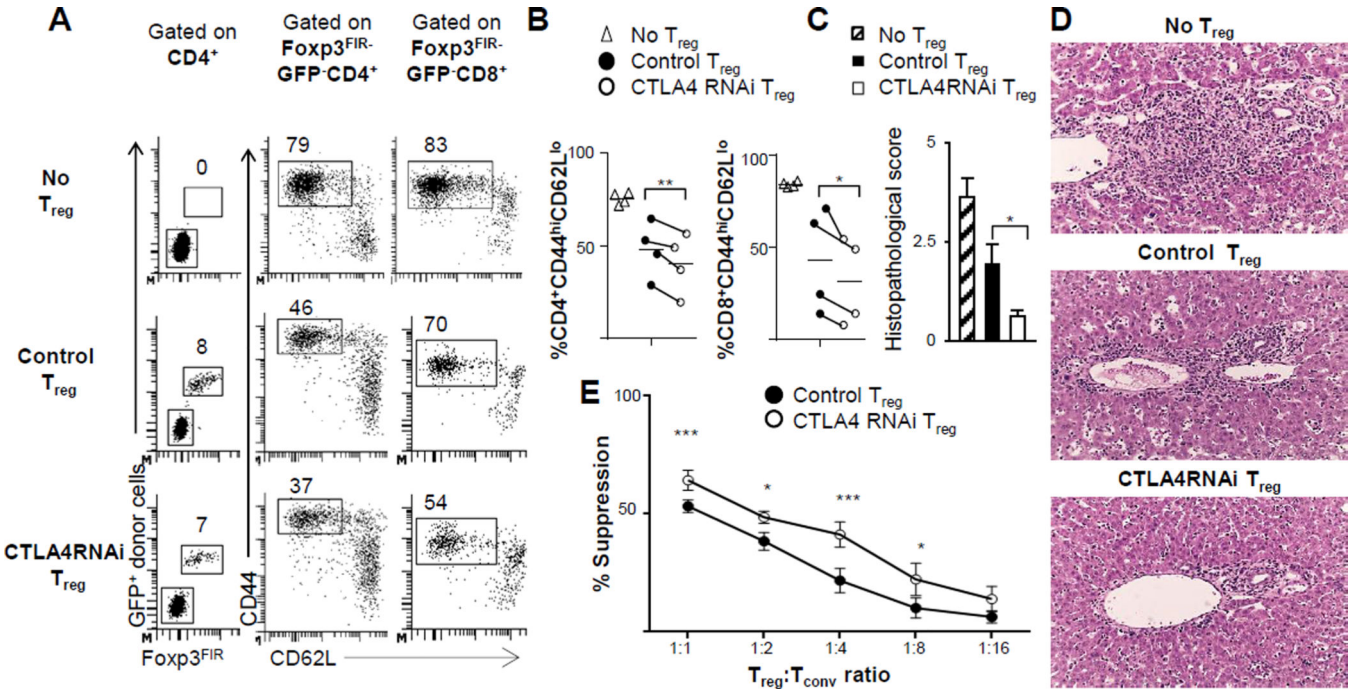

FIGURE 2. The *in vivo* and *in vitro* suppressive function of CD4$^+$Foxp3$^+$ T$_{reg}$ cells was not compromised but rather enhanced by a modest reduction in CTLA4 expression

(**A**) Flow cytometry plots of the spleen of B6.*Foxp3^{sf}* mice reconstituted with naïve T$_{reg}$ cells from CTLA4RNAi or PL4 vector control donors. Donor T$_{reg}$ cells were marked with ubiquitously expressed GFP in the PL4 and CTLA4RNAi transgenic lines (numbers represent percentages of gated CD4$^+$ and CD8$^+$ populations). (**B**)*In vivo* suppression of CD4$^+$ and CD8$^+$ T-cell activation determined by analyses of the CD44^{hi}CD62L^{low} subset. Each data-point represents one animal (line indicating average of the group). (**C–D**) Histopathological scores and representative H&E sections of the livers of the B6.*Foxp3^{sf}* mice reconstituted with T$_{reg}$ cells (original magnification: x12.5) assessed for lymphocytic infiltration (n=4 per group from 4 independent experiments; Mean ± SEM). (**E**) Summarized results from *in vitro* T$_{reg}$ suppression assays (n=5 from 3 independent experiments; Mean ± SEM). Control T$_{reg}$ cells were from transgene-negative littermates or age- & sex-matched PL4 vector transgenic mice. *p<0.05; **p<0.01; ***p<0.005.

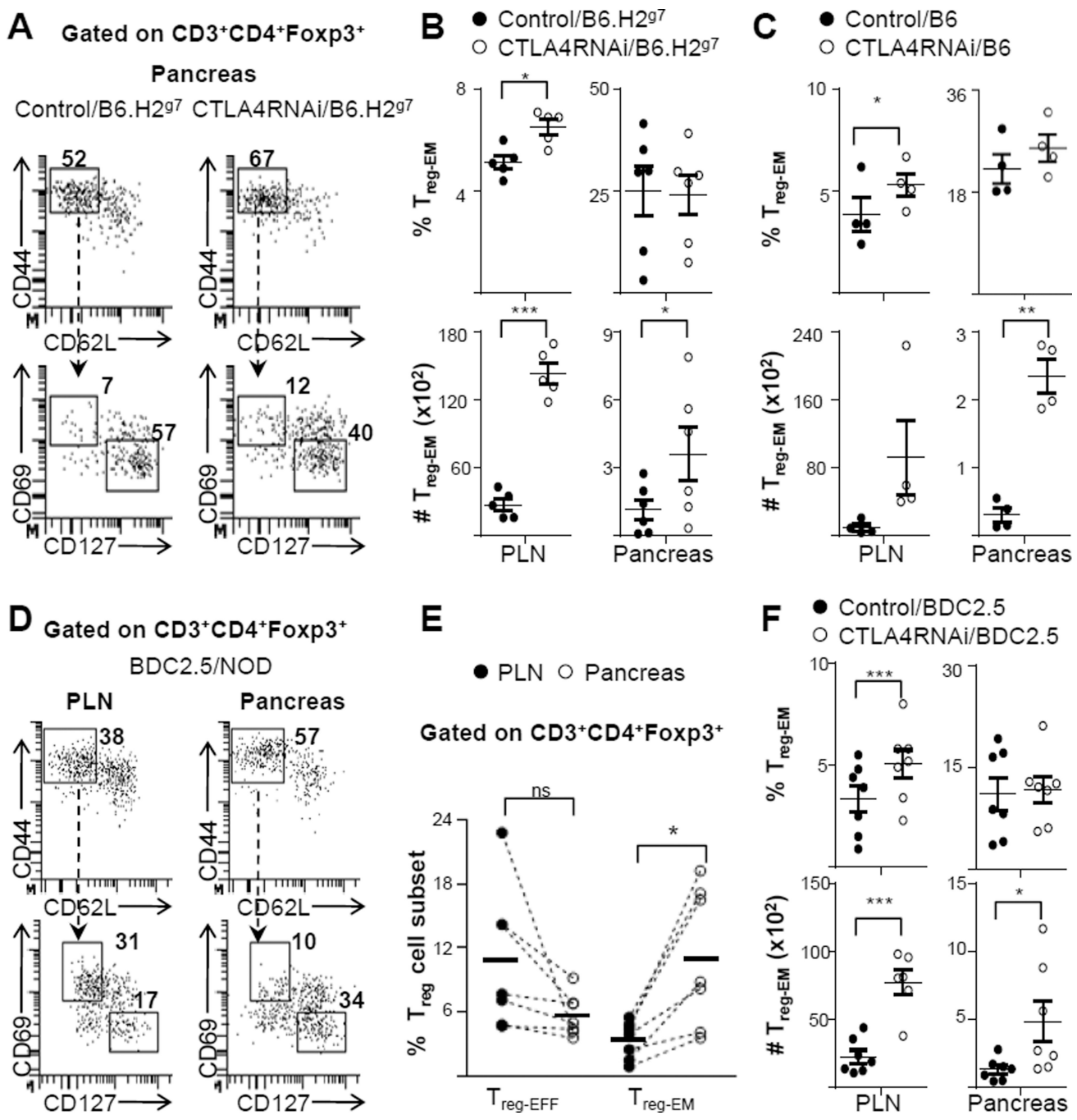

FIGURE 3. CTLA4 reduction increased effector memory formation of T_{reg} cells in the target tissue of mice on diverse genetic backgrounds

(**A**) Flow cytometry analyses of the $T_{reg\text{-}EFF}$ and $T_{reg\text{-}EM}$ subsets in the pancreas (numbers represent percentages of gated T_{reg} populations). (**B**) Frequencies and total cell numbers of the $CD4^+$ $T_{reg\text{-}EM}$ subset with CTLA4RNAi or transgene-negative littermate controls on the B6.H2^{g7} background (n=5–6 per group, 4–12 week old; Mean ± SEM). (**C**) Analyses of mice on the B6 background. Control data represent a pool of transgene-negative littermates or age- & sex-matched PL4 vector transgenic mice (n=4 per group, 9–16 week old; Mean ±

SEM). (**D**) Flow cytometry plots of the PLN and pancreas in BDC2.5/NOD mice showing auto antigen-specific $T_{reg\text{-}EFF}$ and $T_{reg\text{-}EM}$ subsets (numbers represent percentages of gated T_{reg} populations). (**E**) Comparison of the frequencies of antigen-specific $CD4^+$ $T_{reg\text{-}EM}$ and $CD4^+$ $T_{reg\text{-}EFF}$ subsets in the tissue and the draining lymph nodes of BDC2.5/NOD mice (n=7 per group; line indicating average of the group). (**F**) Frequencies and total cell numbers of the auto antigen-specific $T_{reg\text{-}EM}$ subset impacted by CTLA4 modulation. Control data represent a pool of CTLA4RNAi-transgene-negative littermate BDC2.5 mice or age- & sex-matched PL4/BDC2.5 mice (n=6–7 per group, 7–12 week old; Mean ± SEM). Each data-point represents one animal. *p<0.05; **p<0.01; ***p<0.005; ns, not significant.

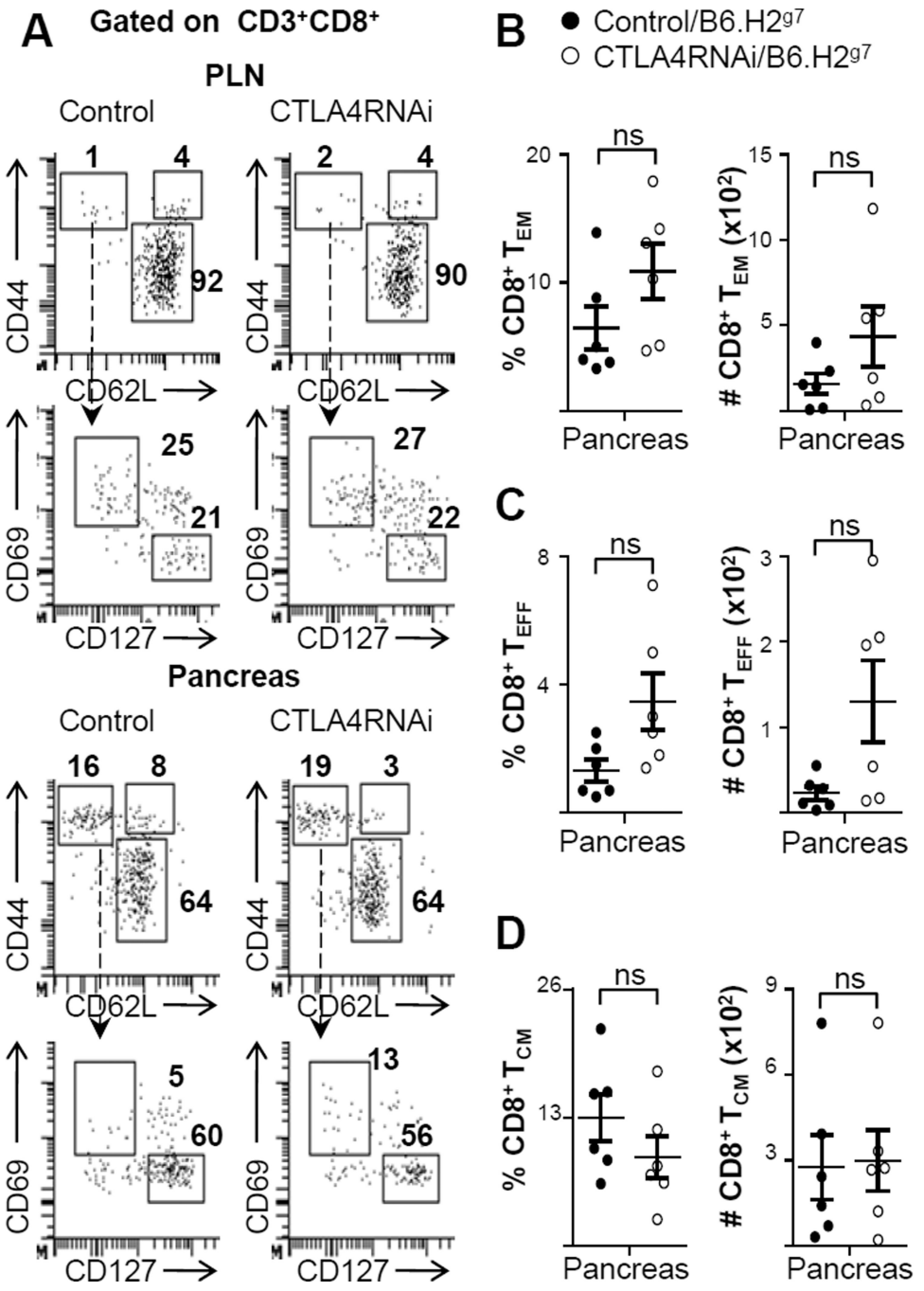

FIGURE 4. Little impact of a modest reduction of CTLA4 on CD8$^+$ T cell memory in the target tissue

(**A**) Flow cytometry analyses of the naïve, T_{CM}, T_{EFF} and T_{EM} subsets of the conventional CD8$^+$ T cell compartment in the pancreas and PLN (numbers represent percentages of gated CD8$^+$ population). (**B–D**) Frequencies and total cell numbers of CD8$^+$ T_{EM} (**B**), CD8$^+$ T_{EFF} (**C**) and CD8$^+$ T_{CM} (**D**) subsets impacted by CTLA4RNAi on the B6.H2^{g7} background. Control mice were transgene-negative littermates (n=6 per group, 4–12 week old). Each data-point represents one animal (Mean ± SEM). ns, not significant.

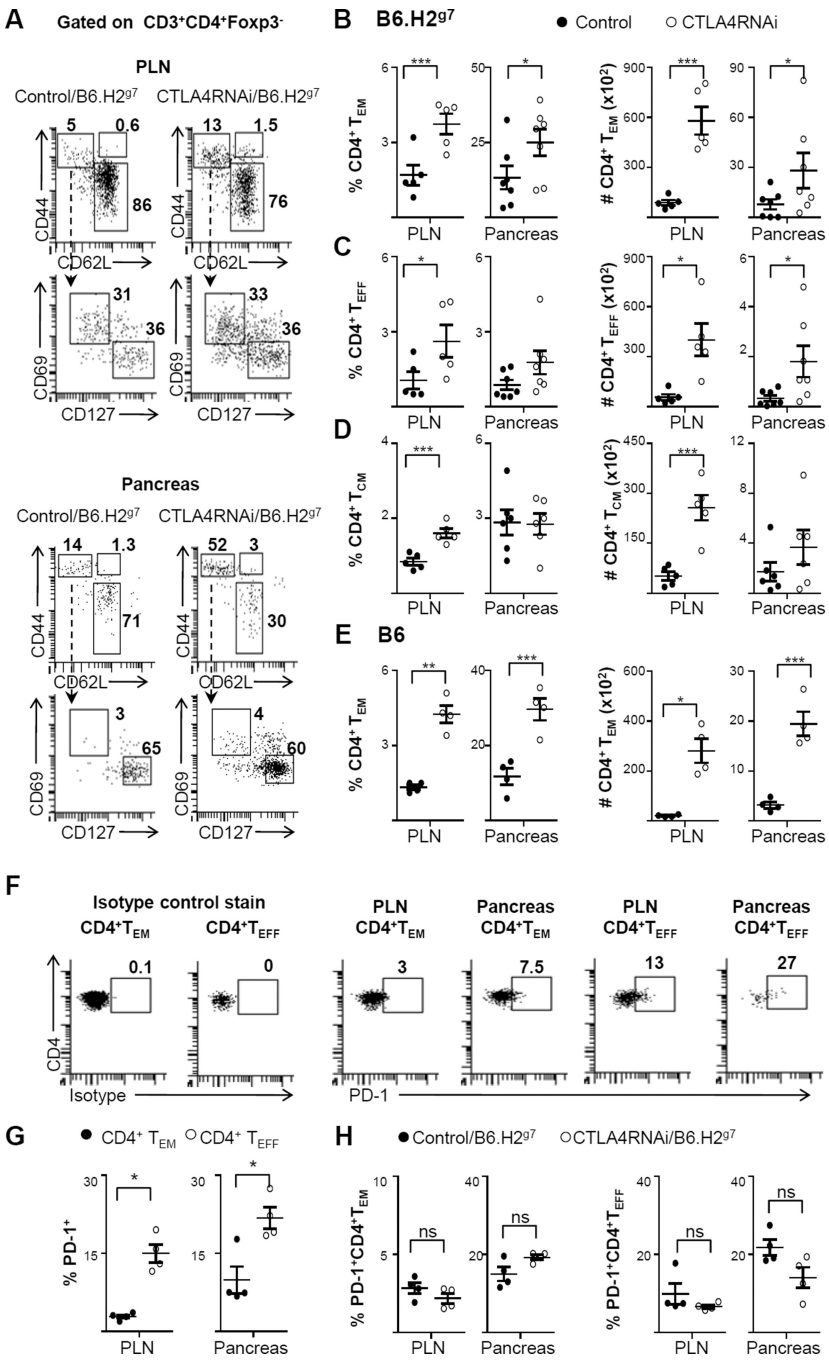

FIGURE 5. CTLA4 reduction increased CD4$^+$ effector memory formation in the T_{conv} compartment

(**A**) Flow cytometry analyses of the naïve, T_{CM}, T_{EFF} and T_{EM} subsets of the conventional CD4$^+$ T cell compartment in the PLN and pancreas (numbers represent percentages of gated CD4$^+$ T_{conv} populations). (**B–D**) Frequencies and total cell numbers of CD4$^+$ T_{EM} (**B**), CD4$^+$ T_{EFF} (**C**), CD4$^+$ T_{CM} (**D**) subsets impacted by CTLA4RNAi on the B6.H2^{g7} background. Control mice were transgene-negative littermates (n=5–7 per group, 4–12 week old). (**E**) Frequencies and total cell numbers of CD4$^+$ T_{EM} cells impacted by CTLA4RNAi

on the B6 background. Control data represent a pool of transgene-negative littermates or age- & sex-matched PL4 vector transgenic mice (n=4 per group, 9–16 week old). (**F**) Flow cytometry analyses of the PD-1 expression by $CD4^+$ T_{EFF} and $CD4^+$ T_{EM} subsets (numbers represent percentages of gated $CD4^+$ T_{conv} population). The first two plots show staining with an isotype control antibody of the anti-PD-1 antibody. (**G**) The frequencies of $PD1^+$ cells in the $CD4^+$ T_{EM} and $CD4^+$ T_{EFF} subsets in B6.H2^{g7} mice. (**H**) Effects of CTLA4 reduction on the frequencies of $PD1^+CD4^+T_{EM}$ and $PD1^+CD4^+T_{EFF}$ subsets on the B6.H2^{g7} background. Control mice were transgene-negative littermates (n=4 per group, 12–17 week old). Each data-point represents one animal (Mean ± SEM). *p<0.05; **p<0.01; ***p<0.005; ns, not significant.

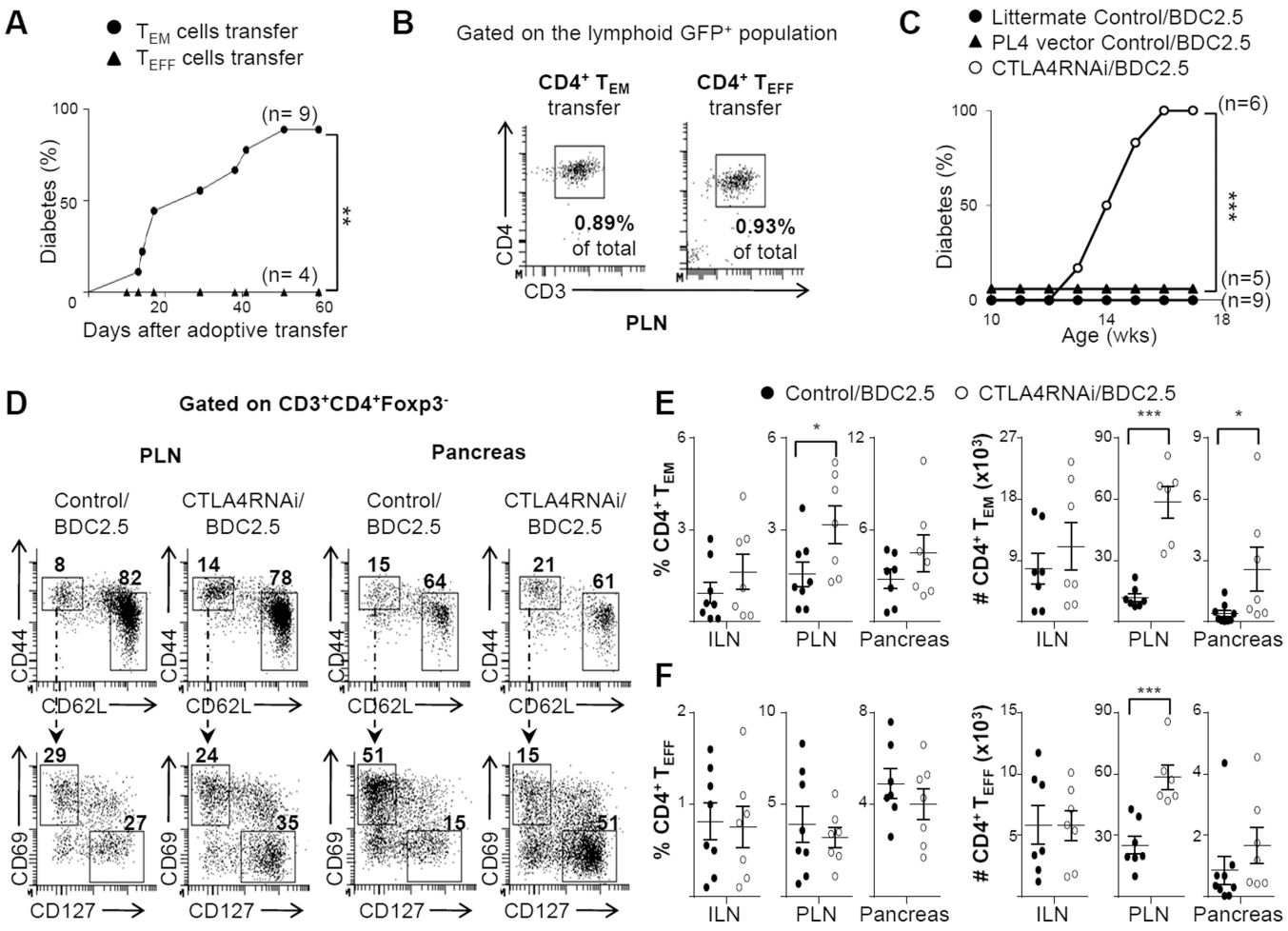

FIGURE 6. CTLA4 reduction promoted formation of auto antigen-specific CD4$^+$ effector memory cells but not effectors

(**A**) Purified β-cell auto antigen-specific T_{EFF} or T_{EM} cells from the spleen of the BDC2.5/NOD.Foxp3^{FIR} mice carrying the PL4 vector transgene (GFP$^+$) were adoptively transferred into NOD.SCID mice. The animals were monitored for diabetes once every 2–3 days, for 60 days. (**B**) Representative flow cytometry plots gated on the lymphoid GFP$^+$ population (the percentage numbers in plot represent the percentage of the gated population in the total PLN cell population analyzed by flow cytometry), showing the CD4$^+$ T_{EM} and CD4$^+$ T_{EFF} subsets that were adoptively transferred into NOD.SCID mice. (**C**) Spontaneous diabetes incidence in BDC2.5/NOD mice with or without CTLA4RNAi, or with the PL4 vector control transgene. (**D**) Flow cytometry analyses of the naïve, T_{EFF} and T_{EM} subsets of the conventional CD4$^+$ T cell compartment in the PLN and pancreas (numbers represent percentages of gated CD4$^+$ T_{conv} population). (**E–F**) Frequencies and total cell numbers of auto antigen-specific CD4$^+$ T_{EM}(**E**) and CD4$^+$ T_{EFF}(**F**) cells in the ILN, PLN and pancreas. Control data represent a pool of CTLA4RNAi-transgene-negative littermate BDC2.5 mice or age- & sex-matched PL4/BDC2.5 mice (n=7–9 mice per group). Each data-point represents one animal (Mean ± SEM). *p<0.05; **p<0.01; ***p<0.005.

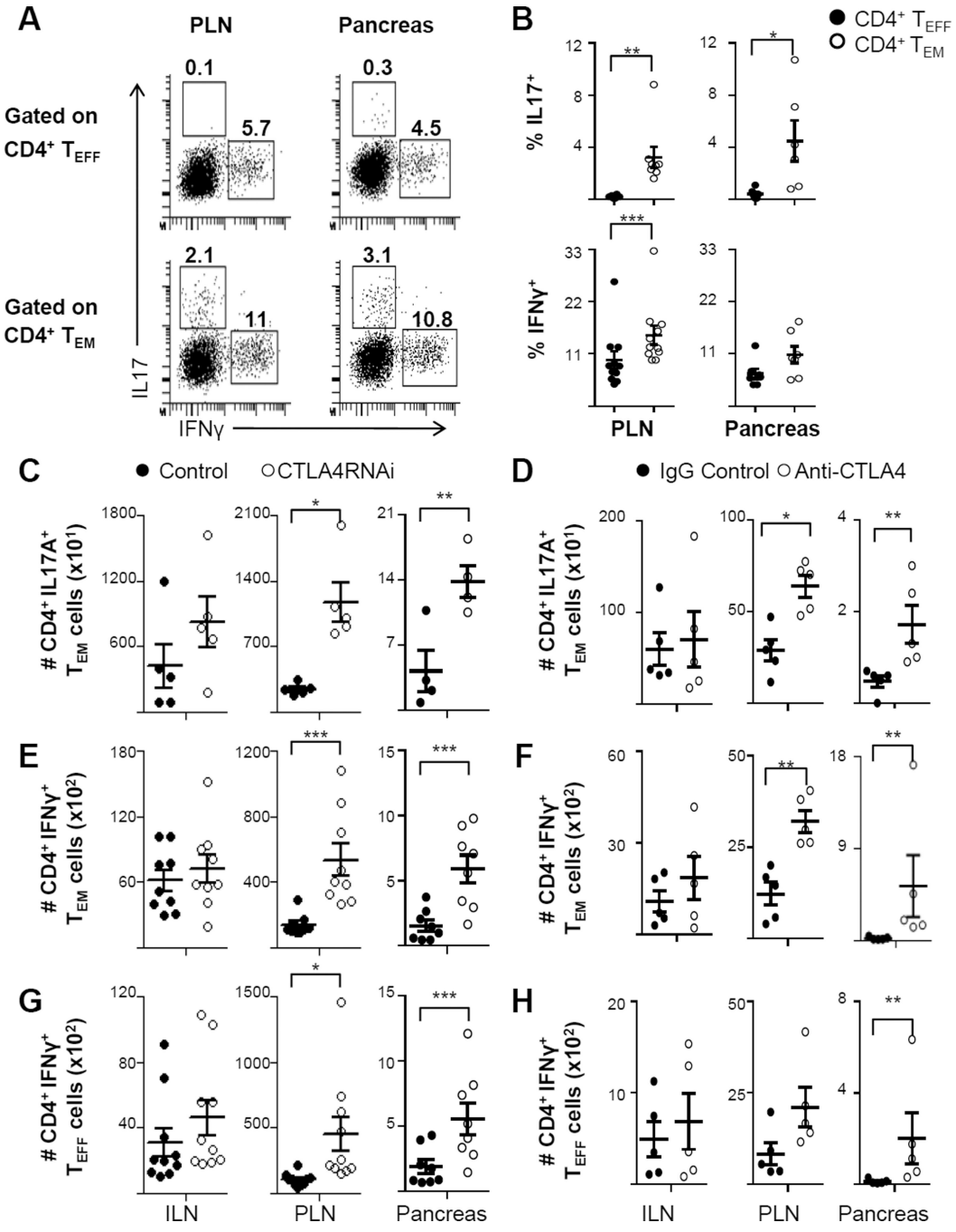

FIGURE 7. CTLA4 down regulation increased IL17 and IFNγ production by auto antigen-specific CD4$^+$ T$_{EM}$ cells

(**A**) Representative intracellular flow cytometry plots of IL17- and IFNγ-producing autoimmune CD4$^+$ T$_{EM}$ and CD4$^+$ T$_{EFF}$ subsets in the PLN and pancreas in BDC2.5/NOD mice (numbers represent percentages of gated populations). (**B**) Frequencies of IL17- and IFNγ-producing autoimmune CD4$^+$ T$_{EFF}$ and CD4$^+$ T$_{EM}$ subsets in the PLN and pancreas in BDC2.5/NOD mice (n=6–11 mice per group). (**C–H**) The effects of CTLA4 modulation by RNAi (**C, E** and **G**) and by antibody treatment (**D, F** and **H**) on IL17-producing autoimmune

$CD4^+$ T_{EM} cells (**C–D**), IFNγ-producing autoimmune $CD4^+$ T_{EM} cells (**E–F**) and IFNγ-producing autoimmune $CD4^+$ T_{EFF} cells (**G–H**) in the ILN, PLN and pancreas. Control data represent a pool of CTLA4RNAi-transgene-negative littermate BDC2.5 mice or age- & sex-matched PL4/BDC2.5 mice (n=4–10 mice per group). Each data-point represents one animal (Mean ± SEM). *p<0.05; **p<0.01; ***p<0.005.

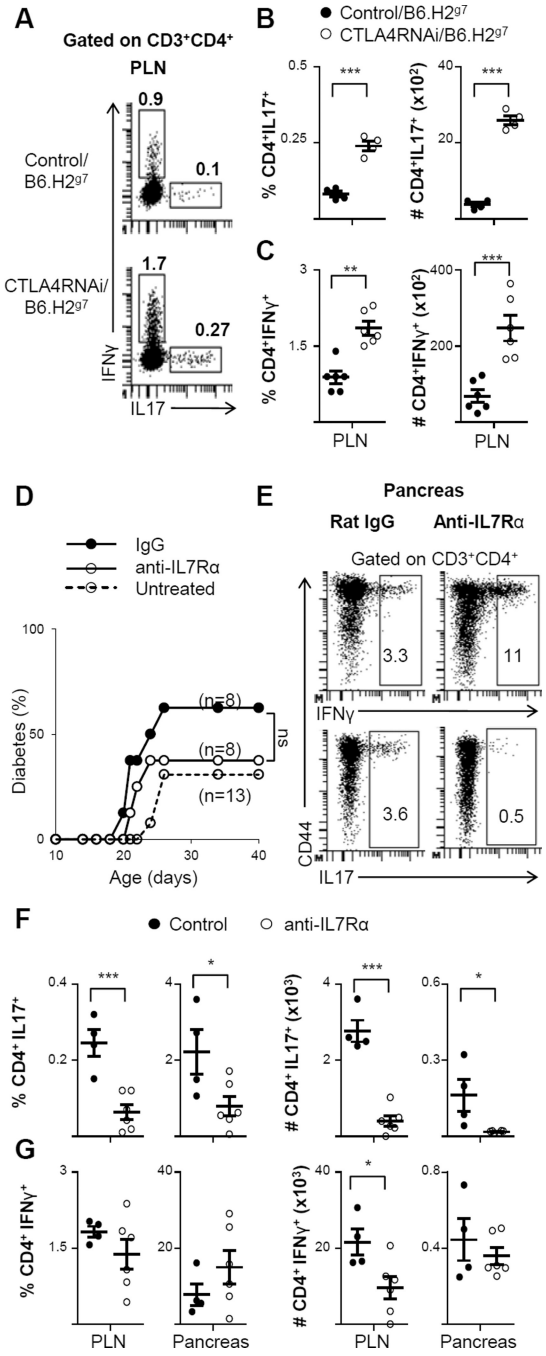

FIGURE 8. Blocking IL7 signaling with anti-IL7Rα antibody treatment suppressed Th17 formation but not diabetes development

(**A**) Representative intracellular flow cytometry plots of IFNγ- and IL17-producing $CD4^+$ T cells in the PLN (numbers represent percentages of gated populations). (**B–C**) Frequencies and total cell numbers of $CD4^+IL17^+$ (**B**) and $CD4^+IFN\gamma^+$ (**C**) subsets impacted by CTLA4RNAi on the $B6.H2^{g7}$ background. Control mice were transgene-negative littermates (n=4–6 per group). (**D**) Littermate CTLA4RNAi/$B6.H2^{g7}$ mice were treated with non-specific ratIgG2a control antibody or anti-IL7Rα antibody for 3 weeks. Mice were

monitored for diabetes for 40 days. (**E**) Representative intracellular flow cytometry plots of the pancreas showing IL17- and IFNγ-production by $CD4^+$ T cells after anti-IL7Rα treatment (numbers represent percentage of gated populations). (**F–G**) Frequencies and total cell numbers of $CD4^+IL17^+$(**F**) and $CD4^+IFN\gamma^+$ (**G**) after anti-IL7Rα treatment (n=4–6 mice per group). Each data-point represents one animal (Mean ± SEM). *p<0.05; **p<0.01; ***p<0.005; ns, not significant.

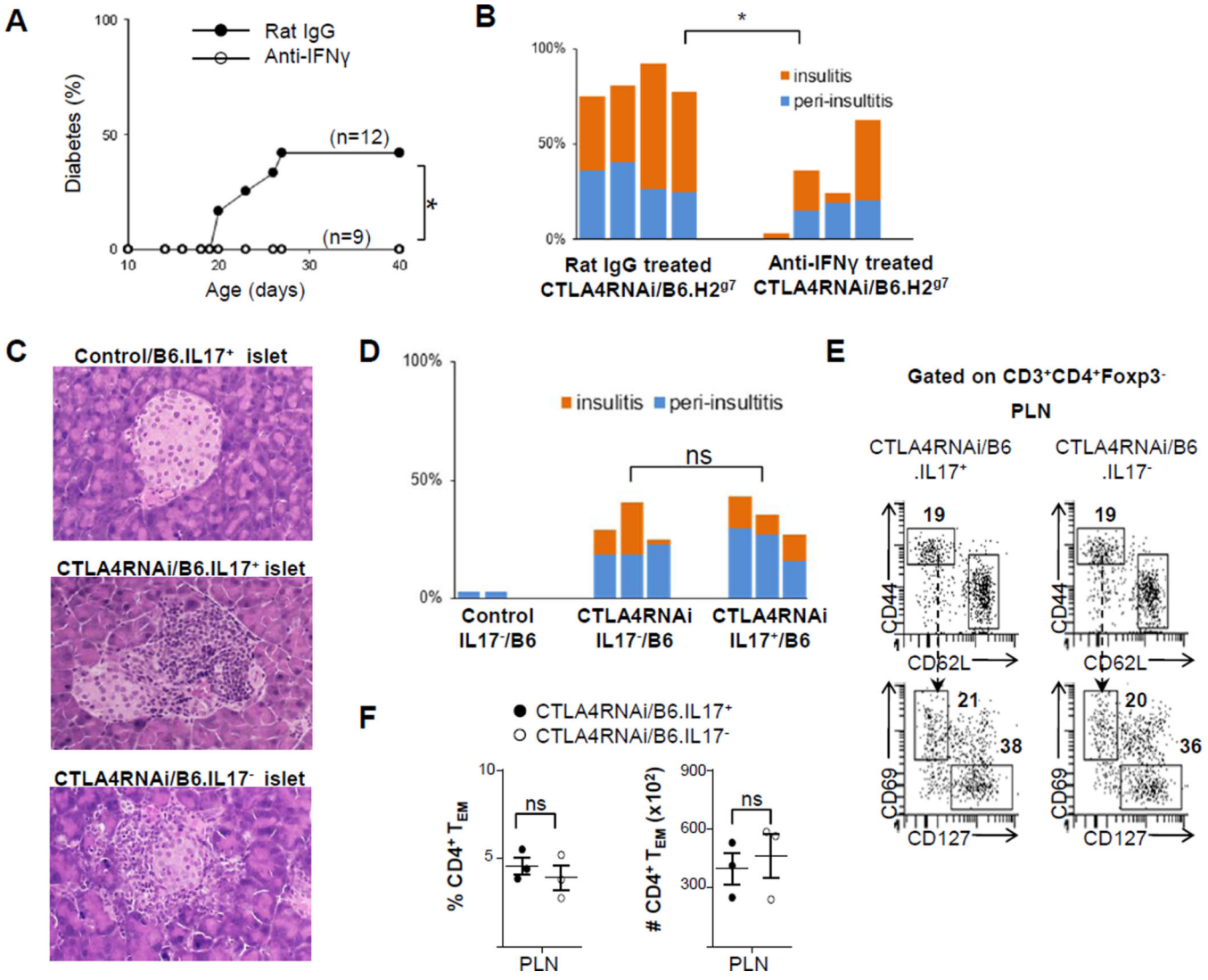

FIGURE 9. Evidence for IFNγ but not IL17 in autoimmune damage to the pancreatic islet caused by CTLA4 down-modulation

(**A**) Effects of anti-IFNγ antibody treatment on diabetes incidence in juvenile CTLA4RNAi/B6.H2^{g7} mice. (**B**) Summary of islet infiltration in anti-IFNγ or control-antibody treated mice (n=4 per group). Each bar represents one animal. (**C**) Representative H&E stained sections of the pancreas from 6-month-old mice on the B6 genetic background (original magnification: x12.5). (**D**) Summary of islet infiltration in 6-month-old mice on the B6 genetic background. Control mice were CTLA4RNAi-transgene-negative littermates. (**E**) Flow cytometry analyses of the T_{EFF} and T_{EM} subsets of the CD4$^+$ T_{conv} cell compartment in the PLN and pancreas (numbers represent percentages of gated CD4$^+$ T_{conv} population). (**F**) Frequencies and total cell numbers of CD4$^+$ T_{EM} subset in IL17$^+$ and IL17$^-$ CTLA4RNAi/B6 mice (n=3 per group). Each data-point represents one animal (Mean ± SEM). *p<0.05; ns, not significant.